

## **7. Results**

The objective of this dissertation was to significantly enhance the existing technology of OFP by changing from sequential hybridization and detection to highly multiplexed hybridizations and simultaneous analysis. This was to be achieved by the use of PNA as hybridization probes and MALDI-TOF MS as means of hybridization detection.

Within the scope of this dissertation several pivotal questions were addressed, such as relevant characteristics of PNA hybridizations and detection as well as the impact of different hybridization parameters. In a multiplex OFP pilot study, a number of selected genomic and cDNA clones was analyzed to assess the feasibility of the innovative concept. Furthermore, potential DNA immobilization systems that allow direct hybridization read-out by MALDI-TOF MS were evaluated in terms of their suitability. In the following experimental results addressing these questions are presented.

### **7.1 Characteristics of PNA hybridizations and MALDI-TOF MS based PNA detection**

#### **7.1.1 Significance of probe length**

Although the use of DNA oligonucleotide probes as short as six nucleotides has been reported (Drmanac et al., 1990, Chechetkin et al., 2000) hybridizations with octamer or shorter DNA probes fail to yield consistent results of sufficient quality. As a consequence, current OFP technology uses degenerated DNA decamer oligonucleotides as hybridization probes which possess an octamer core as informational entity. However, hybridization frequencies of 8mer probes are much lower in practice than the optimal value of 50%. Assuming such a hybridization probability, about 17 probes would be needed for a successful partitioning of 100,000 clones. Calculations of average hybridization frequencies of randomly chosen oligonucleotide probes to random double-stranded target sequences, that are independent from each other and of equal length of 1000 bp, led to the following results: octamers ~ 3%, heptamers ~ 11%, hexamers ~ 39%, and pentamers ~ 86% (Herwig et al., 2000). Yet, these calculations are only approximations since in real experiments neither target DNA is of equal fixed length nor are hybridization probes randomly selected. In practice, a total number of up to 250 octamer probes has to be employed for the characterization of 50,000-100,000 clones to provide for a meaningful OFP analysis (Herwig et al., 1999 and 2000).

PNA, in contrast to DNA, forms duplex hybrids with complementary DNA, (Egholm et al., 1993. Wittung et al., 1994) that show a greater stability compared to DNA/DNA duplexes. Experiments with fluorescence labeled PNA probes suggested that the hybridization of PNA octamers is feasible (Guerasimova et al., 2001). The authors ascribed that finding to the greater PNA/DNA duplex stability which led to the initial assumption that PNA probes even shorter than 8mers can be reliably hybridized. To prove that assumption right, in the course of this dissertation PNA octamer, heptamer and hexamer probes were tested for their informational as well as experimental applicability.

Due to the respectively higher hybridization frequencies of 7mers and 6mers, the use of these probes compared to 8mers was expected to lead to a higher partitioning and hence better clustering of oligonucleotide-fingerprinted clones (Herwig et al., 2000). This expectation could be confirmed by a clustering simulation where the performance of 8mer, 7mer, and 6mer probes in dependence of the maximum sequence length of target DNA was directly compared (fig. 7.1).

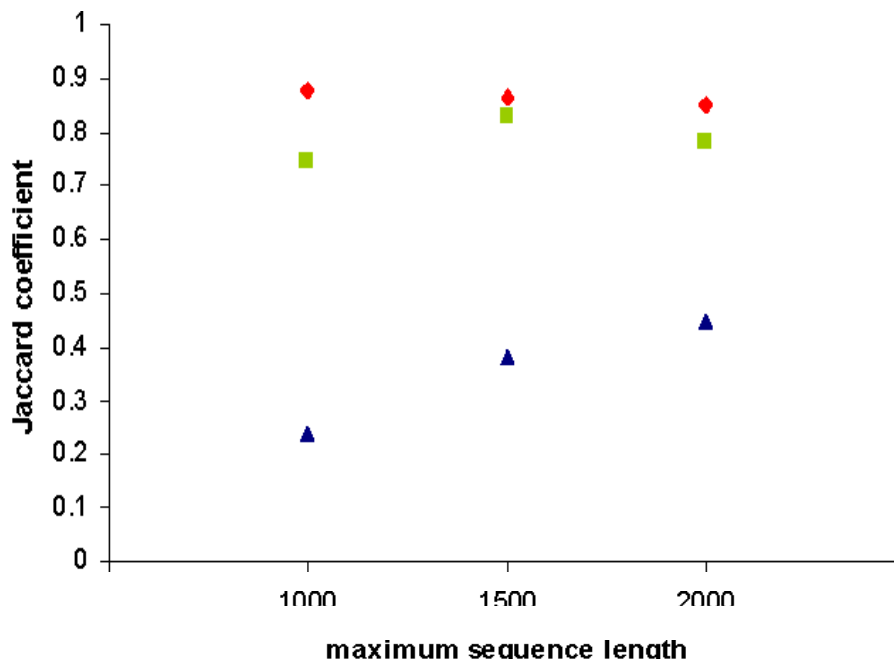


**Figure 7.1 Comparison of clustering quality of 8mer, 7mer, and 6mer probes**

Clustering quality as measured by Jaccard Coefficient (Herwig et al., 1999) was simulated for 70 **8mer**, **7mer** and **6mer** oligonucleotide probes, respectively. A high Jaccard Coefficient reflects a good clustering quality ("1"= perfect clustering). Probes were taken from previously created sets as described in chapter 6.8.1. Target DNA sequences of 300 bp to 1000 bp, 1500 bp, or 2000 bp were generated "in silico" based on Human Brain Unigene set. The experimental noise parameter was set to 20% of false positive/negative hybridization rate.

The comparison of clustering performance clearly demonstrates that, for the given target DNA lengths and oligonucleotide probe number, hexamer and heptamer probes are superior to octamers. Hexamers in turn perform somewhat better than heptamer probes.

To study the impact of varying probe numbers on clustering further simulations were carried out for the better performing 6mers and 7mers (fig. 7.2). From a practical point of view it is impossible to precisely calculate the value of clustering quality due to various

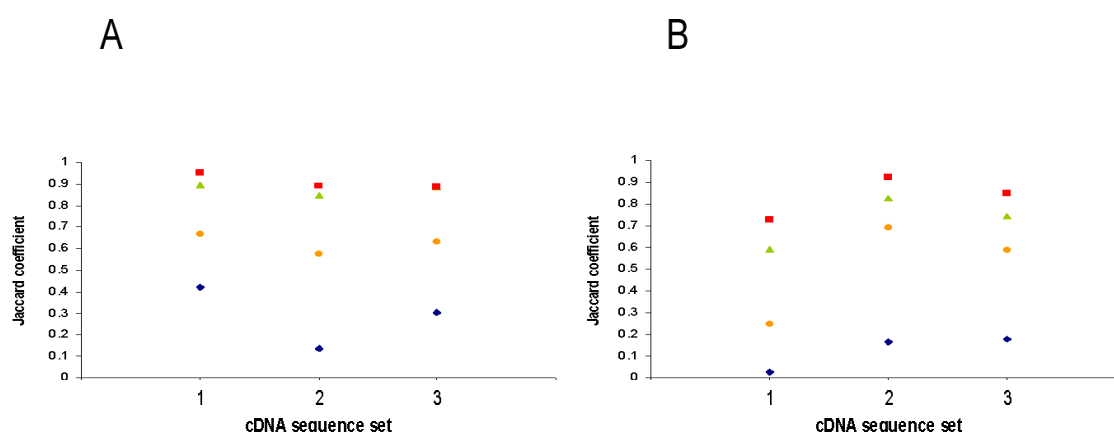


**Figure 7.2 Impact of varying probe numbers on clustering quality**

Clustering quality as measured by Jaccard Coefficient (Herwig et al., 1999) was simulated for three independent sets of about 7000 known cDNA sequences ("in silico" derived from Human Brain Unigene set) each with a length distribution of 300 bp to 2 kb. Simulations were performed with 30, 50, 70, and 100 hexamer (A) or heptamer (B) oligonucleotide probes. These were taken from previously created sets as described in chapter 6.8.1. A high Jaccard Coefficient reflects a good clustering quality ("1"= perfect clustering). The experimental noise parameter was set to 20% of false positive/negative hybridization rate.

experimental sources of error. However, recent successfully completed OFP projects suggest that Jaccard coefficients of at least 0.80 have to be achieved for convincing clustering analyses (empirical observations). Therefore, it can be concluded that 70 hexamer probes are sufficient for a meaningful clustering, whereas for heptamers 100 probes are recommended.

Despite the inferior theoretical partitioning of 8mers all three kinds of oligonucleotides were experimentally examined since hybridization properties of PNA oligonucleotides of these short lengths were unknown in practice and are still unpredictable (SantaLucia et al., 1996). PNA oligonucleotides used for hybridizations were produced as described in chapter 6.8.1. As it was demonstrated that the hybridization of PNA octamers is feasible initial experimental efforts focused on the evaluation of 8mers. Subsequently, 7mer and 6mer probes were also tested for their applicability. Results showed that in principle all

three types can be successfully employed. There was no evidence that 8mers hybridize in a more reliable fashion than 7mers and 6mers, respectively. Neither were hexamer nor heptamer probes more specific as thermodynamic considerations would suggest. However, due to their more favorable desorption and ionization properties, 6mers and 7mers are more easily detected than 8mers in the process of MALDI-TOF MS giving rise to higher absolute signal intensities.

### **7.1.2 Influence of PNA modifications on hybridization and MALDI-TOF MS detection**

Different covalent modifications of PNA have been reported that were introduced to either improve PNA hybridization or MALDI properties. Terminal lysine was shown to have a stabilizing role in PNA/DNA duplexes (Ratilainen et al., 1998) presumably because of an increased PNA strand solubility due to the positively charged lysine residue. The use of O-linker 8-amino-3,6-dioxaoctanoic acid offers the possibility to uniquely mass label and detect PNA probes of similar or identical masses (Griffin et al., 1997). Quaternary ammonium fixed charge-tags were shown to increase the detectability of small DNA oligonucleotides about 100-fold compared to unmodified oligonucleotides employing MALDI-TOF MS (Gut et al., 1997).

To test the influence of the above mentioned modifications on PNA hybridization and MALDI properties, varying numbers of O-linker and lysine residues were incorporated at the N- and C-terminus of PNA octamers. As for a few oligonucleotides, either an O-linker was N-terminally attached, or a lysine residue was C-terminally attached; or both O-linker and lysine were N- and C-terminally attached, respectively, or the octamer sequence was left unmodified. Besides, the impact of different numbers of mass tags (one, three, and five N-terminally attached O-linkers) was examined for octamers. In addition, 8mer, 7mer and 6mer PNA probes were charged-tagged as described in chapter 6.8.2.

As for the incorporation of lysine and/or O-linker, experiments revealed no significant improvement neither in hybridization behavior nor in MALDI-TOF MS detection. For some octamer sequences it appeared as if the N-terminal addition of one O-linker resulted in slightly improved detection compared to unmodified sequences. However, this finding was not consistent and could not be observed for hexamers and heptamers. Probes with larger numbers of N-terminally attached O-linkers (three or five) were consistently found to yield weaker signals - with five O-linkers being worse - suggesting that the process of MALDI is increasingly impaired by the presence of many mass-tags. Although it was not found that the detectability of charged-tagged PNA is noticeably increased as in the case of charge-

tagged DNA oligonucleotides it could be observed that charge-tagging of small PNA oligonucleotides renders them significantly more stable and less prone to fragmentation and alkali adduct formation during the MALDI process (fig. 7.3).

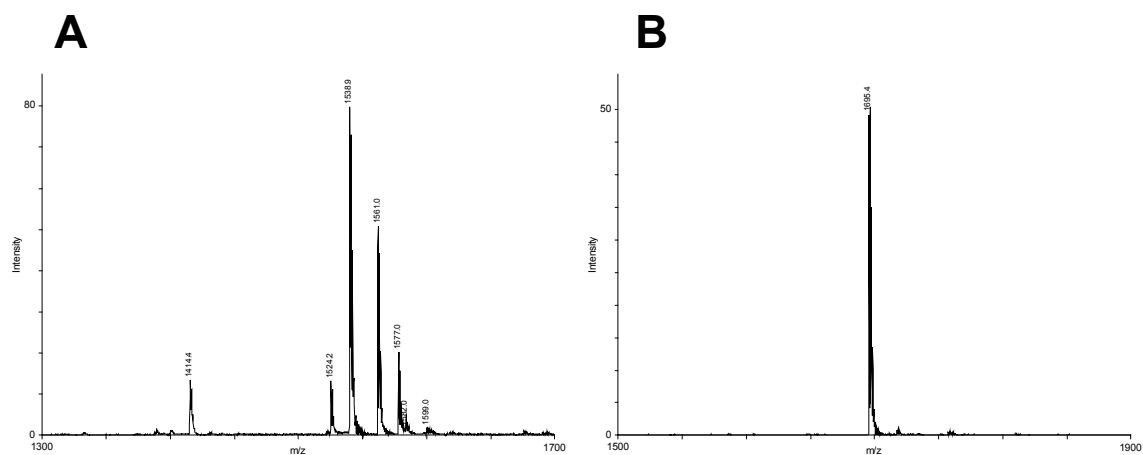


**Figure 7.3** Impact of positive charge-tagging on PNA detection

In a direct comparison, a PNA hexamer was left unmodified (**A**) and positively charged-tagged (**B**), before being subjected to analysis by MALDI-TOF MS. In the spectra, relative signal intensity (intensity) as a function of mass-to-charge ratio ( $m/z$ ) is shown. Charge-tagging of PNA was performed as described in chapter 6.8.2.

### 7.1.3 Determination of total probe number and creation of PNA sets

The determination of the total number of PNA probes that can be hybridized and detected simultaneously is of utmost importance as it ultimately defines the degree of multiplexing and hence the capacity of the concept of multiplexed OFF.

Little has been reported so far about multiplexed PNA hybridizations. In their MALDI-TOF MS approach to the analysis of genetic variations Griffin et al. (1997) successfully applied duplex PNA hybridizations and detected up to five PNA probes of unique mass in parallel. Furthermore, Ross et al. (1997) demonstrated that it is even feasible to hybridize four PNA probes simultaneously.

To address the issue of multiplexing in PNA hybridizations it was tested how many PNA probes can be resolved in one spectrum in an meaningful fashion. Furthermore, hybridization studies were carried out with different pools of varying probe numbers to evaluate at which degree of multiplexing meaningful results are still to be obtained.

Due to the experimental expertise gained for PNA octamers, the performance of these PNA oligonucleotides was investigated first. Preliminary experiments carried out

with up to 57 different PNA octamer probes, however, revealed their poor hybridization and MALDI properties and showed that, for PNA octamers, the applied degree of multiplexing (57 probes) was too high for sufficient signal resolution and hence analyzable hybridization results. Further experiments were performed with PNA hexamers and heptamers. In contrast to PNA octamers, these showed higher theoretical partitioning and superior desorption and ionization properties. Since for 8mers a total probe number of over fifty resulted in insufficient signal resolution, no additional efforts were made to exceed this figure. As for 6mers and 7mers, global sets were created comprising all respective available PNA that fitted in with respect to their individual mass and mass resolution. In addition, sets consisting of lower numbers of different PNA probes were designed according to their individual MALDI properties (so-called "subsets"), i.e. probes were grouped that, on an equimolar basis, yielded signal intensities of comparative absolute values. The compositions of the respective sets are given in chapter 5.7. To compare resolution and detection sensitivity of highly multiplexed PNA 6mer and 7mer pools, the two global sets of 40 different PNA hexamers and heptamers were directly analyzed by MALDI-TOF MS (fig. 7.4). It appears that hexamers of this number can be

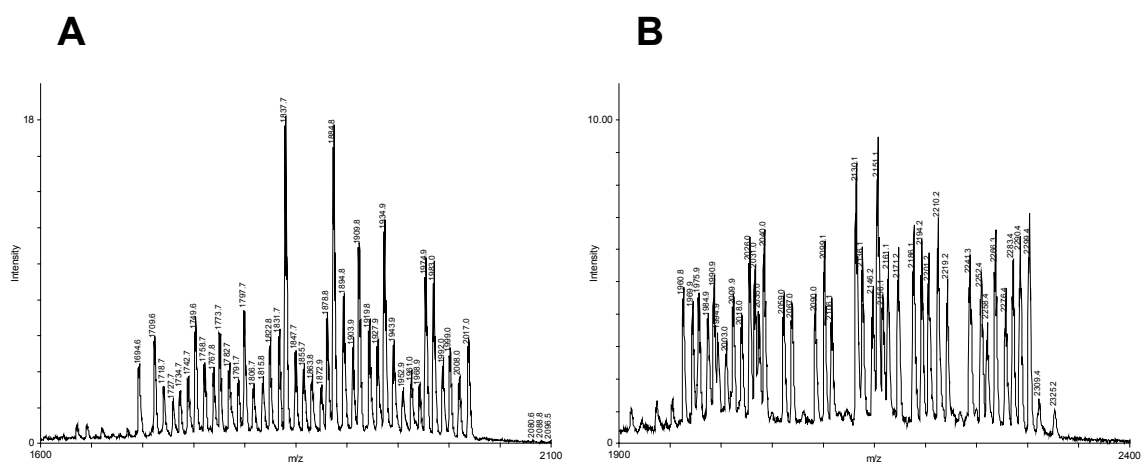


**Figure 7.4 Parallel detection of 40 different PNA hexamers and heptamers**

40 different PNA hexamers and heptamers (PNA sets "6mer global" and "7mer global") were detected simultaneously by MALDI-TOF MS. Experimental probe masses are annotated. Compositions of the respective sets including PNA names are given in chapter 5.7. Each PNA was applied at a concentration of 667 nM.

slightly better resolved than heptamers. Both overall resolution and signal intensities were found to be significantly higher compared to those obtained for octamers. The better performance is probably due to the superior MALDI properties of 6mers and 7mers. Regarding detection, it can be concluded that for PNA hexamer and heptamer probes an

up to 40-plex approach is feasible. Comprehensive hybridization studies comprising PNA 6mer and 7mer global sets as well as all subsets are presented in chapter 7.3.

### 7.2 Impact of different parameters on PNA hybridization

Beside the study of impact of overall probe number, multiplexed PNA hybridizations were carried out to examine PNA hybridization properties and optimize hybridization conditions towards better specificity. Experiments were performed in tube format as described in chapter 6.8.3.1. Basic experimental conditions were 20 mM Tris-HCl (pH 8,0) as buffer and 1,5 h as duration of hybridization. Shorter periods (0,5 h) led to weaker results. Longer periods (4 h, 8 h, 16 h) did not yield higher signal intensities nor did they improve specificity. Although first insight on PNA hybridization properties was gained by the use of short synthetic oligonucleotides, the comprehensive examinations presented here were performed with PCR amplified DNA inserts of four different genomic clones. This was because longer PCR products show secondary structure thereby epitomizing target DNA as in “real” OFP projects. As PNA probes, both hexamers and heptamers were tested employing charge-tagged PNA sets “6mer sub1” and “7mer sub2” (refer to chapter 5.7 for composition).

#### 7.2.1 Influence of probe and target DNA concentration

The influence of individual and global probe concentration as well as target DNA concentration on hybridization results was examined for all available 6mer and 7mer PNA sets. As for the study of individual probe concentration, probe sets were created of which all respective concentrations were brought into line with each other, i.e. relative PNA signal intensities were equalized (“equalized set”). In the case of PNA set “6mer global”, for instance, the originally weakest PNA was up to eighteen times more concentrated than the PNA originally yielding strongest signals. In addition, all PNA probes of a respective set were employed in an equimolar fashion (“equimolar set”). Either sets were applied in hybridization experiments by which four different genomic clones were analyzed. Figure 7.5 shows the highly reproducible hybridization results of both an equalized and an equimolar PNA hexamer set with two of these genomic clones. The results clearly demonstrate that altered individual probe concentrations have virtually no impact on PNA presence and signal intensity. PNA probes showing moderate signal intensities in pure PNA mixes may be of highest signal intensities in hybridization spectra and vice versa – as indicated by red arrows for PNA 6P008 - strongly suggesting that hybridization results

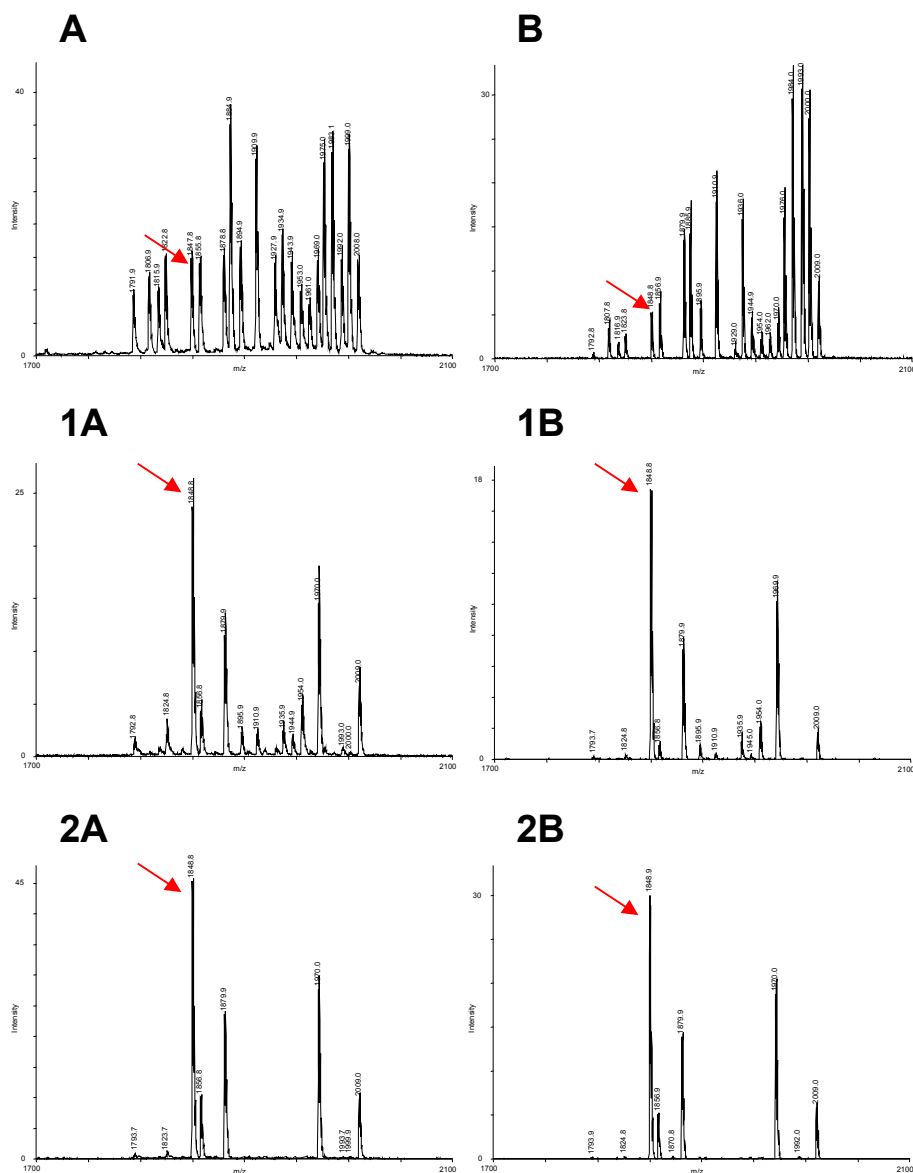


**Figure 7.5 Impact of altered individual probe concentration on hybridization**

Four genomic clones were hybridized with equalized PNA set “6mer sub1” (**A**) and an equimolar version (**B**) of it. As for the former, the originally weakest PNA was four times more concentrated than the PNA originally yielding strongest signals. Pure PNA mixes are depicted (**A**, **B**) as well as reproducible hybridization results gained with both mixes and two different clones (**1A**, **1B**, **2A**, **2B**). Experimental probe masses are annotated and the relative peak heights of PNA 6P008 is indicated by red arrows. The composition of PNA set “6mer sub1” is given in chapter 5.7.

are target DNA sequence-dependent. Since the alteration of individual probe concentration did neither affect presence nor intensity of PNA signals only equimolar PNA sets were applied for all subsequent hybridization experiments. In a further study the impact of global PNA concentration on hybridization was examined (fig. 7.6). Again, four different genomic clones were analyzed by hybridizing PNA sets of varying equimolar concentration (1333 nM, 667 nM, 333 nM, and 167 nM). The illustration shows that



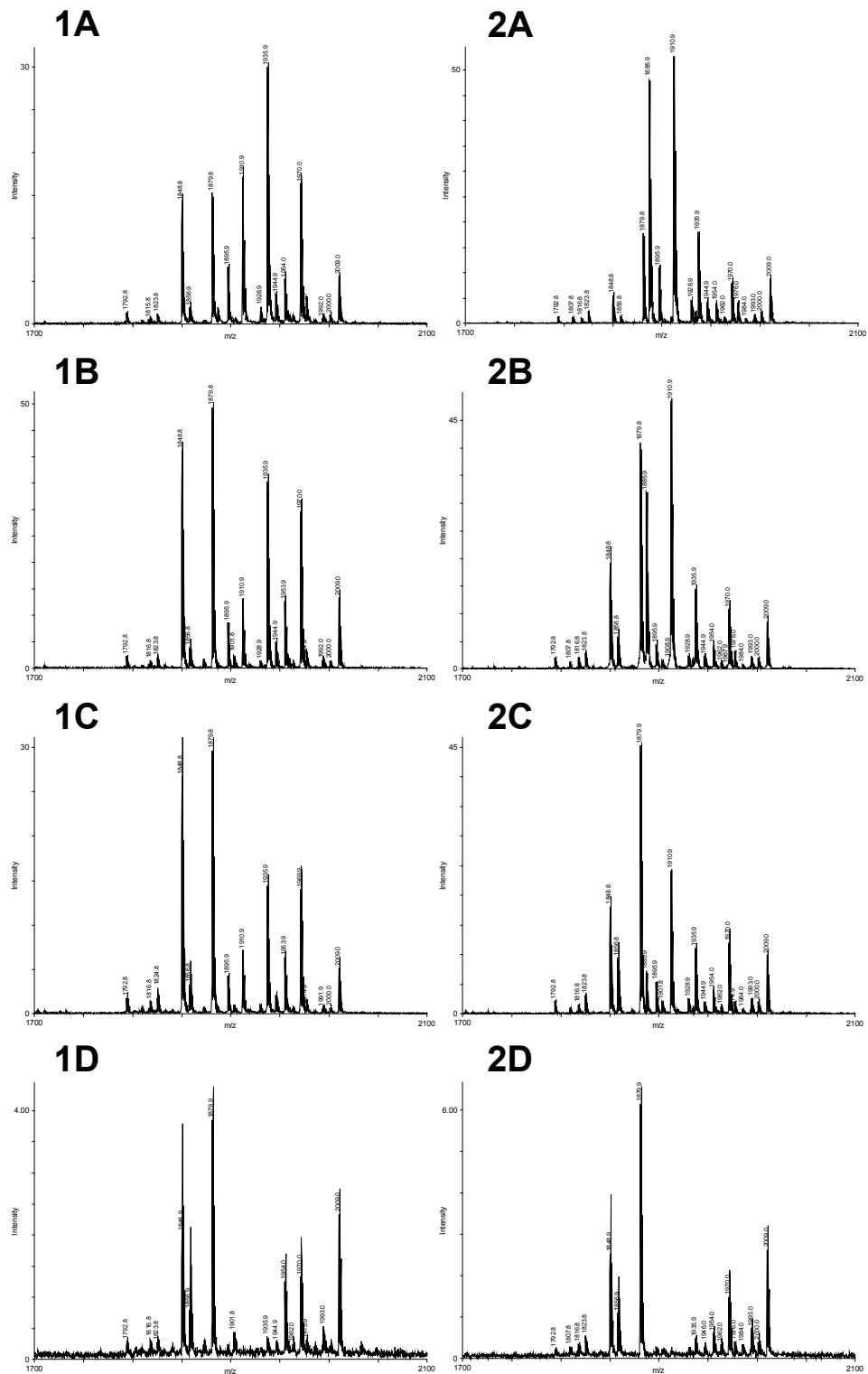


**Figure 7.6 Impact of global probe concentration on hybridization**

Four genomic clones were hybridized with equimolar PNA set “6mer sub1” of varying global concentrations (**A**: 1333 nM, **B**: 667 nM, **C**: 333 nM, **D**: 167 nM). Reproducible hybridization results gained with all four concentrations and two of the clones are depicted (**1A-D**, **2A-D**). Experimental probe masses are annotated. The composition of PNA set “6mer sub1” is given in chapter 5.7. Target DNA was applied at a concentration of 56 nM.

hybridization profiles, i.e. presence and respective signal intensities of probes, are dependent on global probe concentrations. Lower concentrations (fig 7.6: 1D, 2D) gave rise to hybridization spectra of inferior quality that appear to be less distinguishable. Higher concentrations may unexpectedly alter the overall hybridization profile (fig. 7.6: 1A) and are - from an economical point of view - more costly. Due to inconsistent performance no meaningful information with regard to global PNA concentration could be derived for heptamers. As a compromise and to ensure hybridization results of sufficient quality, a global PNA concentration of 667 nM was used as standard for both hexamers and heptamers in subsequent experiments.

Beside individual and global probe concentrations the influence of target DNA concentration on hybridization was also investigated. Figure 7.7 demonstrates that, analogous to the global concentration of probes, hybridization profiles depend very much on overall target DNA concentration. In fact, it appears as if DNA concentration affects hybridization even more critically as is suggested by the prevalent change of hybridization profile through all tested concentrations (fig 7.7: 1A-D, 2A-D). To ensure a sufficient degree of quality, a target DNA concentration of 56 nM was chosen as standard for subsequent hybridization experiments.

### 7.2.2 Influence of additives and temperature

Elevated temperatures and/or the addition of certain chemicals have been reported to influence the outcome of desoxy- and ribonucleic acid hybridizations towards higher specificity. However, rather little is known for PNA hybridizations.

Within the scope of the dissertation several promising substances have been tested to examine their impact on PNA hybridization and to optimize hybridization conditions towards higher specificity. Furthermore, the impact of temperature on its own as well as in combination with some of these substances was explored. The substances tested comprise sodium chloride, tetramethyl- and tetraethylammonium chloride (TMACl, TEACl), formamide, betaine, sodium N-lauroyl-sarcosine, SDS, and Tween-20.

Sodium chloride has been described to lower  $T_m$  in DNA duplexes (Marmur and Doty, 1962) as well as to increase specificity in PNA oligomer array based hybridizations (Weiler et al., 1997). Tetramethyl- and tetraethylammonium salts bind to AT-rich DNA regions thereby abolishing the preferential melting of AT versus GC base pairs (Klump, 1997, Orosz and Wetmur, 1977). Formamide has been known for decades as a DNA melting agent inducing stringency in hybridizations (Bonner et al., 1967, McConaughy et al., 1969) whereas betaine is suggested to reduce the formation of secondary structure caused by

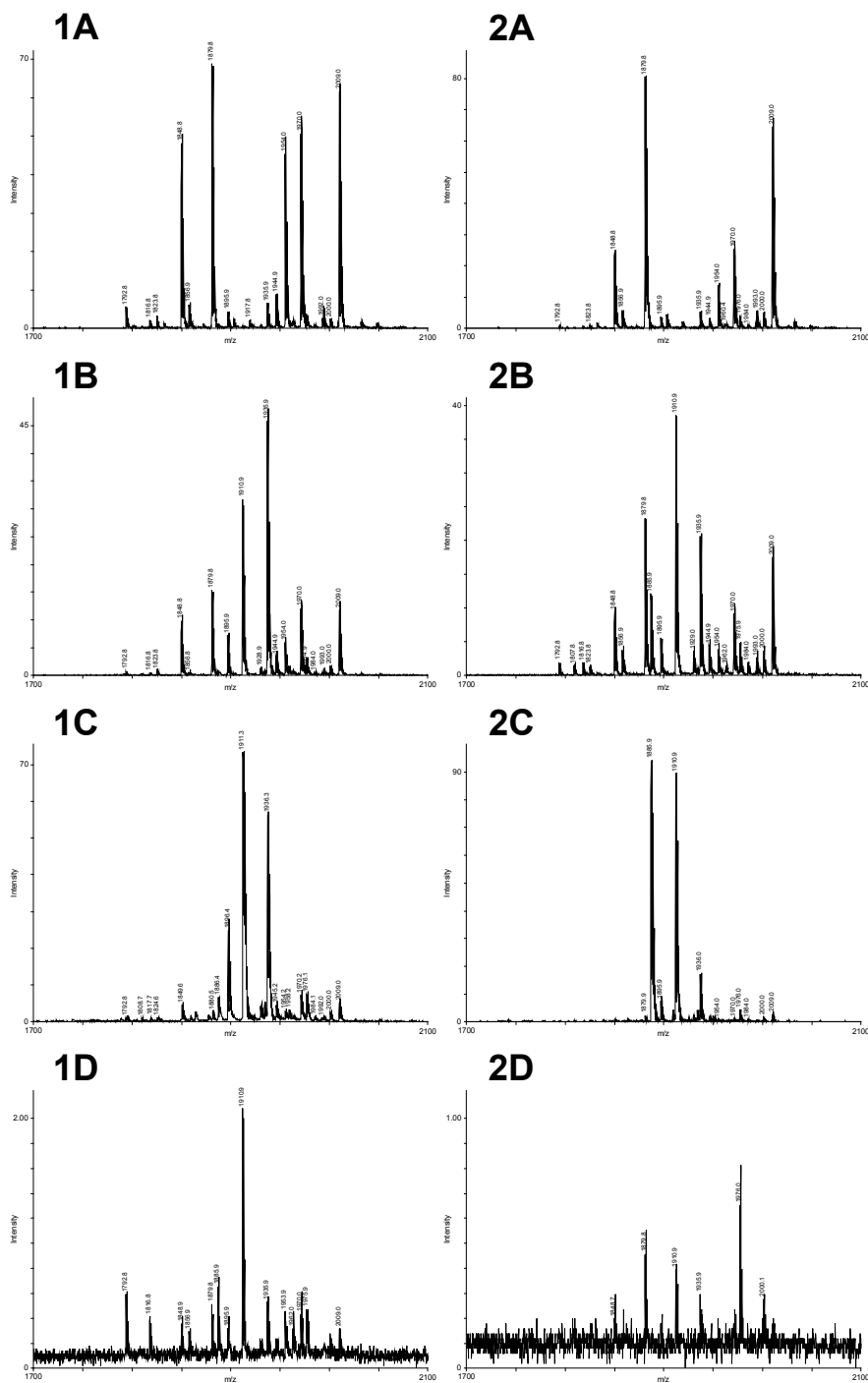


**Figure 7.7 Impact of target DNA concentration on hybridization**

Four genomic clones were hybridized with equimolar PNA set “6mer sub1” and varying concentrations of target DNA (**A**: 112 nM, **B**: 56 nM, **C**: 28 nM, **D**: 14 nM). Reproducible hybridization results gained with all four concentrations and two of the clones are depicted (**1A-D**, **2A-D**). Experimental probe masses are annotated. The composition of PNA set “6mer sub1” is given in chapter 5.7. Each PNA was applied at a concentration of 667 nM.

GC-rich regions (Henke et al., 1997), a phenomenon exploited primarily in PCR. The addition of detergents, such as sodium N-lauroyl-sarcosine, SDS, and Tween-20, has

been shown to reduce unspecificity in various membrane-based techniques applying any class of probe.

Sodium chloride, TMACI, TEACI, and betaine were tested at concentrations of 20 mM, 50 mM, 200 mM, and 500 mM. The impact of formamide was examined with 0%, 10%, 20%, and 30% (v/v) formamide added whereas 0.2%, 0.5%, 1% and 2% (v/v) of respective detergent were applied. In addition, the influence of formamide, betaine and a combination of both in dependence of temperature was explored. Of the tested substances only formamide showed a favorable impact (fig 7.8). All others did affect results in a rather unfavorable way if there was an impact at all, i.e. overall signal intensities were decreased without a concomitant increase in specificity. The addition of detergents even introduced an extra experimental source of error due to heavy foam formation. As expected beforehand and confirmed by the experiments illustrated in figure 7.8 formamide induces a melting of DNA duplexes rendering target DNA more

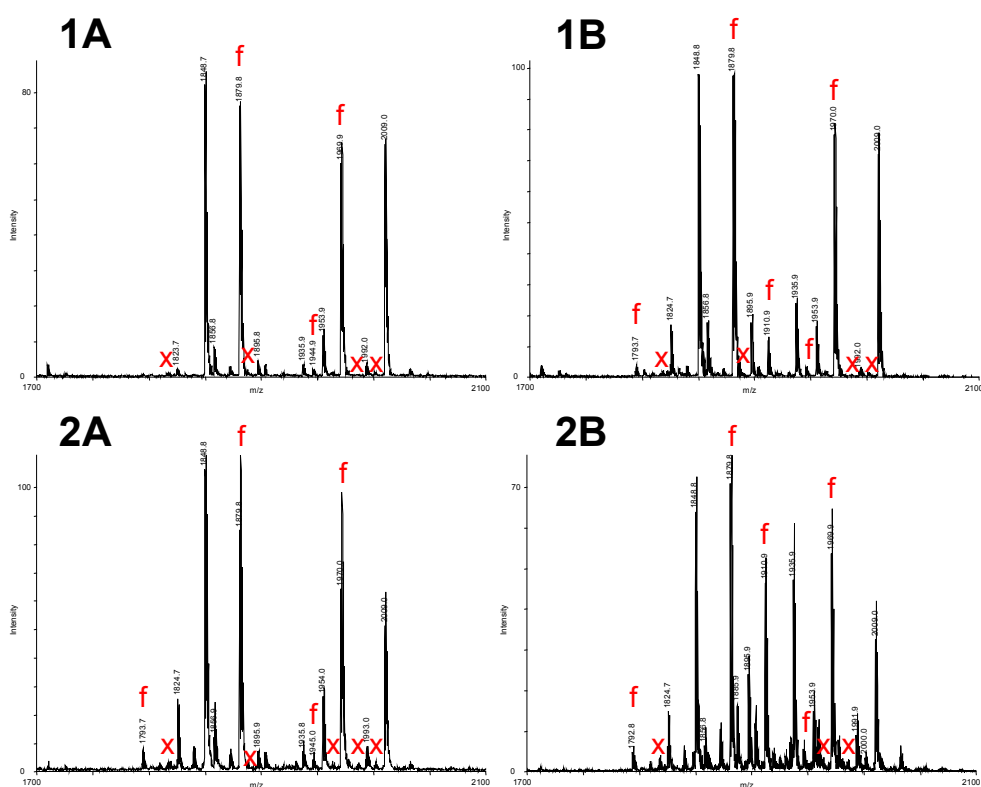


**Figure 7.8 Impact of the addition of formamide on hybridization**

Four genomic clones were hybridized with equimolar PNA set “6mer sub1” and varying concentrations of formamide [0%, 10%, 20%, 30% (v/v)]. Reproducible hybridization results gained with either no formamide (**A**) or 10% (v/v) formamide (**B**) added and two of the clones are depicted (**1A**, **1B**, **2A**, **2B**). A red “f” stands for a PNA hybridized as false positive, whereas a red “x” represents a missing true positive PNA. Experimental probe masses are annotated. The composition of PNA set “6mer sub1” is given in chapter 5.7. Each PNA was applied at a concentration of 667 nM, target DNA was applied at 56 nM.

accessible to hybridization probes. This is documented by the increase of PNA signal diversity (fig. 7.8: 1B, 2B) compared to hybridization spectra obtained with no additional formamide (fig. 7.8: 1A, 2A). Although it initially appears that extra unspecificity is introduced (slight increase in false positive rate) originally missing true positive PNA probes are also gained. As a consequence, it was decided to include formamide [10% (v/v)] as standard additive for all subsequent hybridizations. Heptamers, however, did not show to be affected to the same extent by the presence of formamide, i.e. the strong melting effect observed for hexamers could not be seen.

In a further study the impact of temperature on hybridization in the presence of 10% (v/v) formamide was examined. In the range from 25° C to 50° C temperature was tested in 5° C steps. Figure 7.9 clearly demonstrates that the elevation of hybridization temperature does not lead to more specificity but to drastically deteriorated hybridization profiles, i.e. presence and respective intensity of PNA signals. At 50° C hybridization temperature, for instance, many true positive PNA probes are missing whereas three prominent false positives still persist (fig. 7.9: 1C, 2C). Similar results were obtained for heptamers which showed a slightly better hybridization reliability at elevated temperatures. Therefore, it was decided to employ 35° C as standard hybridization temperature for 6mers and 40° C as a standard for 7mers.

### **7.3 Multiplexed OFP analysis of selected clones of known sequence**

For a comprehensive evaluation of their hybridization properties PNA hexamers and heptamers were tested in different sets as described in chapter 7.1.3. Within the course of a pilot study, a number of selected genomic as well as cDNA clones of known sequence was analyzed by means of these PNA sets to demonstrate the "proof of principle" of the concept of multiplexed OFP. Hybridizations were carried out for 1,5 h in the presence of 10% (v/v) formamide at 35° C (6mers) and 40° C (7mers). Target DNA was applied at a concentration of 56 nM, each PNA was hybridized at a concentration of 667 nM. Due to persisting PNA unspecificity results were analyzed on the basis of individual hybridization profiles as described in chapter 6.10.

#### **7.3.1 Analysis of genomic DNA clones**

31 sequence-confirmed genomic DNA clones, that are void of repeat regions, were analyzed by hybridization to prevent artifacts and hence additional sources of experimental error. These 31 clones fall into five clusters of different size and two cluster-

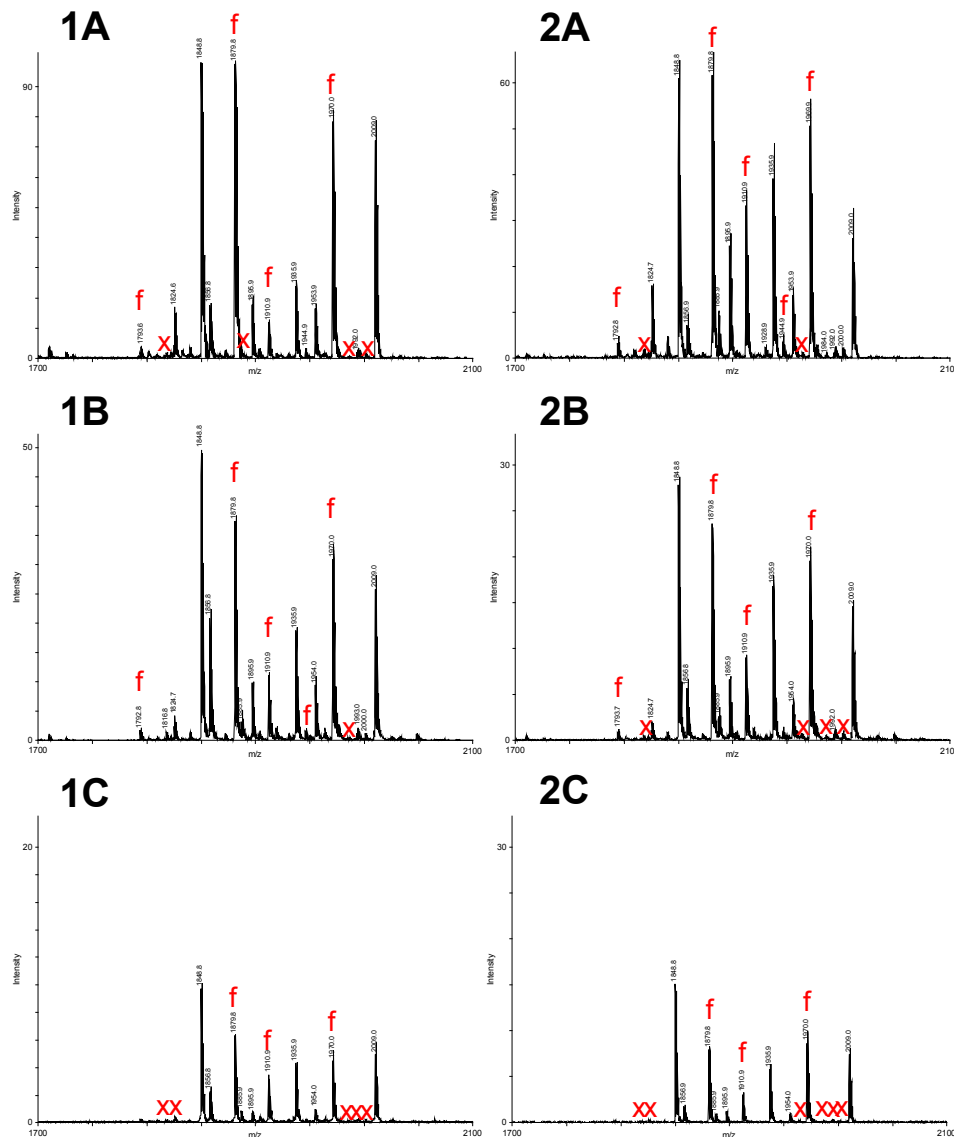


**Figure 7.9 Impact of temperature on hybridization in the presence of formamide**

Four genomic clones were hybridized with equimolar PNA set “6mer sub1” at varying temperatures (25° C, 30° C, 35° C, 40° C, 45° C, 50° C) in the presence of 10% (v/v) formamide. Reproducible hybridization results gained with two of the clones at 35° C (A), 45° C (B), and 50° C (C) hybridization temperature are depicted (1A-C, 2A-C). A red “f” stands for a PNA hybridized as false positive, whereas a red “x” represents a missing true positive PNA. Experimental probe masses are annotated. The composition of PNA set “6mer sub1” is given in chapter 5.7. Each PNA was applied at a concentration of 667 nM, target DNA was applied at 56 nM.

independent singletons. All clones were hybridized with the available PNA 6mer and 7mer subsets. Out of these 31 clones, 14 clones were additionally hybridized with both PNA 6mer and 7mer global set in an approach to determine the practical limit of multiplexing. Figure 7.10 shows the outcome of that approach. With either probe length no convincing data could be gained. It appears that clones belonging to the same cluster are as randomly correlated as are unrelated ones. Figure 7.11 exhibits original mass spectra of,

7. Results

**A**

Cl. A	F21	H14	J20	O21	Cl. C	C14	M10	N07					
<b>F21</b>	<b>0,9667</b>	<b>H14</b>	<b>0,9623</b>	<b>J20</b>	<b>0,9829</b>	<b>O21</b>	<b>0,9091</b>	<b>C14</b>	<b>0,9696</b>	<b>M10</b>	<b>0,9641</b>	<b>N07</b>	<b>0,9914</b>
P06	0,9632	C14	0,9331	O21	<b>0,4086</b>	<b>H14</b>	<b>0,9088</b>	L24	0,9560	P06	0,9501	L24	0,9733
P19	0,9551	N07	0,9297	<b>H14</b>	<b>0,3890</b>	N07	0,8978	<b>N07</b>	<b>0,9472</b>	P19	0,9493	E14	0,9527
E14	0,9454	L24	0,9227	N07	0,3836	L24	0,8972	P19	0,9453	<b>N07</b>	<b>0,9440</b>	F13	0,9477
M10	0,9344	<b>O21</b>	<b>0,9088</b>	L24	0,3601	C14	0,8964	L11	0,9399	E14	0,9405	<b>C14</b>	<b>0,9472</b>
D11	0,9321	M10	0,9058	C14	0,3483	M10	0,8746	D11	0,9390	L24	0,9381	D11	0,9450
L11	0,9209	L11	0,9042	F13	0,3328	D11	0,8705	E14	0,9388	<b>C14</b>	<b>0,9370</b>	<b>M10</b>	<b>0,9440</b>
F13	0,9196	D11	0,8898	L11	0,3290	E14	0,8620	<b>M10</b>	<b>0,9370</b>	F21	0,9344	L11	0,9423
C14	0,9132	E14	0,8819	M10	0,3267	L11	0,8572	H14	0,9331	L11	0,9339	P19	0,9410
L24	0,9059	P19	0,8781	E14	0,3253	F13	0,8476	P06	0,9264	D11	0,9337	P06	0,9322
N07	0,8955	F13	0,8644	D11	0,3212	P19	0,8468	F13	0,9185	F13	0,9231	H14	0,9297
<b>H14</b>	<b>0,8415</b>	P06	0,8524	P19	0,3084	P06	0,8286	F21	0,9132	H14	0,9058	O21	0,8978
<b>O21</b>	<b>0,8198</b>	<b>F21</b>	<b>0,8415</b>	P06	0,3033	<b>F21</b>	<b>0,8198</b>	O21	0,8964	O21	0,8746	F21	0,8955
<b>J20</b>	<b>0,2787</b>	<b>J20</b>	<b>0,3890</b>	<b>F21</b>	<b>0,2787</b>	<b>J20</b>	<b>0,4086</b>	J20	0,3483	J20	0,3267	J20	0,3836

Cl. D	D11	E14	F13	L11	Cl. E	L24	P06	P19					
<b>E14</b>	<b>0,9787</b>	<b>E14</b>	<b>0,9943</b>	<b>F13</b>	<b>0,9814</b>	<b>L11</b>	<b>0,9799</b>	<b>L24</b>	<b>0,9917</b>	<b>P06</b>	<b>0,9866</b>	<b>P19</b>	<b>0,9846</b>
<b>D11</b>	<b>0,9770</b>	<b>F13</b>	<b>0,9807</b>	<b>E14</b>	<b>0,9807</b>	P19	0,9538	N07	0,9733	<b>P19</b>	<b>0,9757</b>	<b>P06</b>	<b>0,9757</b>
<b>F13</b>	<b>0,9656</b>	<b>D11</b>	<b>0,9787</b>	<b>D11</b>	<b>0,9656</b>	<b>E14</b>	<b>0,9529</b>	C14	0,9560	F21	0,9632	E14	0,9601
P19	0,9474	P06	0,9632	N07	0,9477	N07	0,9423	<b>P19</b>	<b>0,9520</b>	E14	0,9632	F21	0,9551
P06	0,9461	P19	0,9601	P06	0,9446	<b>D11</b>	<b>0,9413</b>	E14	0,9410	M10	0,9501	L11	0,9538
N07	0,9450	<b>L11</b>	<b>0,9529</b>	P19	0,9386	C14	0,9399	M10	0,9381	D11	0,9461	<b>L24</b>	<b>0,9520</b>
<b>L11</b>	<b>0,9413</b>	N07	0,9527	<b>L11</b>	<b>0,9321</b>	P06	0,9391	D11	0,9371	F13	0,9446	M10	0,9493
C14	0,9390	F21	0,9454	L24	0,9238	M10	0,9339	<b>P06</b>	<b>0,9357</b>	L11	0,9391	D11	0,9474
L24	0,9371	L24	0,9410	M10	0,9231	<b>F13</b>	<b>0,9321</b>	L11	0,9304	<b>L24</b>	<b>0,9357</b>	C14	0,9453
M10	0,9337	M10	0,9405	F21	0,9196	L24	0,9304	F13	0,9238	N07	0,9322	N07	0,9410
F21	0,9321	C14	0,9388	C14	0,9185	F21	0,9209	H14	0,9227	C14	0,9264	F13	0,9386
H14	0,8898	H14	0,8819	H14	0,8644	H14	0,9042	F21	0,9059	H14	0,8524	H14	0,8781
O21	0,8705	O21	0,8620	O21	0,8476	O21	0,8572	O21	0,8972	O21	0,8286	O21	0,8468
J20	0,3212	J20	0,3253	J20	0,3328	J20	0,3290	J20	0,3601	J20	0,3033	J20	0,3084

**B**

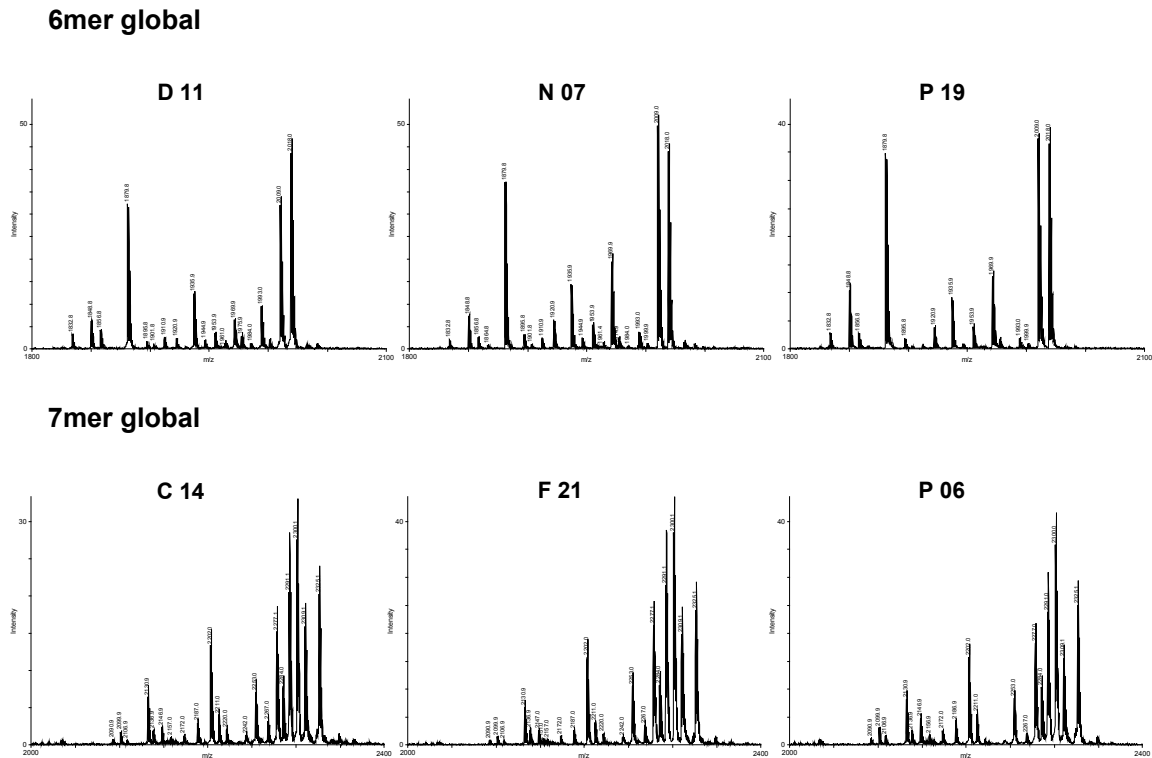
Cl. A	F21	H14	J20	O21	Cl. C	C14	M10	N07					
<b>F21</b>	<b>0,9903</b>	<b>H14</b>	<b>0,9683</b>	<b>J20</b>	<b>0,9820</b>	<b>O21</b>	<b>0,9616</b>	<b>C14</b>	<b>0,9928</b>	<b>M10</b>	<b>0,9730</b>	E14	0,9132
<b>C14</b>	<b>0,9815</b>	M10	0,9299	M10	0,9503	F21	0,9419	<b>F21</b>	<b>0,9815</b>	J20	0,9503	<b>N07</b>	<b>0,9126</b>
L11	0,9713	<b>J20</b>	<b>0,9291</b>	F13	0,9370	L11	0,9391	P06	0,9650	H14	0,9299	P19	0,9003
P06	0,9682	F13	0,9287	P19	0,9353	C14	0,9190	L11	0,9536	F13	0,9074	<b>C14</b>	<b>0,8859</b>
P19	0,9476	<b>O21</b>	<b>0,8973</b>	C14	0,9345	P19	0,9178	P19	0,9464	<b>C14</b>	<b>0,9000</b>	J20	0,8852
O21	0,9419	P19	0,8732	<b>H14</b>	<b>0,9291</b>	<b>J20</b>	<b>0,9176</b>	E14	0,9420	O21	0,8906	<b>F21</b>	<b>0,8814</b>
E14	0,9316	F21	0,8656	E14	0,9287	P06	0,9147	J20	0,9345	<b>F21</b>	<b>0,8876</b>	P06	0,8786
J20	0,9260	C14	0,8566	F21	0,9260	F13	0,9028	O21	0,9190	E14	0,8807	F13	0,8694
L24	0,9034	L24	0,8535	<b>O21</b>	<b>0,9176</b>	<b>H14</b>	<b>0,8973</b>	L24	0,9107	P19	0,8801	D11	0,8571
<b>M10</b>	<b>0,8876</b>	E14	0,8514	P06	0,9069	E14	0,8921	<b>M10</b>	<b>0,9000</b>	L24	0,8667	O21	0,8413
F13	0,8872	D11	0,8501	D11	0,8961	M10	0,8906	<b>N07</b>	<b>0,8859</b>	P06	0,8607	<b>M10</b>	<b>0,8300</b>
<b>N07</b>	<b>0,8814</b>	L11	0,8454	L11	0,8901	L24	0,8815	F13	0,8852	D11	0,8579	L11	0,8278
H14	0,8656	P06	0,8392	L24	0,8893	N07	0,8413	H14	0,8566	L11	0,8514	H14	0,8272
D11	0,8379	N07	0,8272	N07	0,8852	D11	0,8304	D11	0,8523	<b>N07</b>	<b>0,8300</b>	L24	0,7898

Cl. D	D11	E14	F13	L11	Cl. E	L24	P06	P19					
<b>D11</b>	<b>0,9542</b>	<b>E14</b>	<b>0,9710</b>	<b>F13</b>	<b>0,9786</b>	<b>L11</b>	<b>0,9904</b>	<b>L24</b>	<b>0,9617</b>	F21	0,9682	<b>P19</b>	<b>0,9657</b>
<b>F13</b>	<b>0,9366</b>	P19	0,9455	J20	0,9370	F21	0,9713	C14	0,9107	C14	0,9650	F21	0,9476
<b>E14</b>	<b>0,9107</b>	C14	0,9420	<b>D11</b>	<b>0,9366</b>	C14	0,9536	F21	0,9034	<b>P06</b>	<b>0,9650</b>	C14	0,9464
P19	0,8990	F21	0,9316	H14	0,9287	P06	0,9505	L11	0,8998	L11	0,9505	E14	0,9455
J20	0,8961	J20	0,9287	P19	0,9269	O21	0,9391	J20	0,8893	<b>P19</b>	<b>0,9349</b>	J20	0,9353
M10	0,8579	P06	0,9199	<b>E14</b>	<b>0,9158</b>	P19	0,9193	<b>P19</b>	<b>0,8867</b>	E14	0,9199	<b>P06</b>	<b>0,9349</b>
N07	0,8571	<b>F13</b>	<b>0,9158</b>	M10	0,9074	L24	0,8998	<b>P06</b>	<b>0,8843</b>	O21	0,9147	F13	0,9269
C14	0,8523	N07	0,9132	O21	0,9028	J20	0,8901	F13	0,8817	J20	0,9069	L11	0,9193
H14	0,8501	<b>D11</b>	<b>0,9107</b>	F21	0,8872	<b>E14</b>	<b>0,8785</b>	O21	0,8815	<b>L24</b>	<b>0,8843</b>	O21	0,9178
F21	0,8379	O21	0,8921	C14	0,8852	<b>F13</b>	<b>0,8564</b>	M10	0,8667	N07	0,8786	N07	0,9003
L24	0,8325	M10	0,8807	L24	0,8817	M10	0,8514	H14	0,8535	F13	0,8670	D11	0,8990
O21	0,8304	<b>L11</b>	<b>0,8785</b>	N07	0,8694	H14	0,8454	E14	0,8515	M10	0,8607	<b>L24</b>	<b>0,8867</b>
P06	0,8231	L24	0,8515	P06	0,8670	N07	0,8278	D11	0,8325	H14	0,8392	M10	0,8801
<b>L11</b>	<b>0,7834</b>	H14	0,8514	<b>L11</b>	<b>0,8564</b>	<b>D11</b>	<b>0,7834</b>	<b>N07</b>	<b>0,7898</b>	D11	0,8231	H14	0,8732

**Figure 7.10 Correlation analysis of genomic DNA clones hybridized with global PNA sets**

14 genomic DNA clones were analyzed by hybridization with PNA sets “6mer global” (A) and “7mer global” (B), respectively. Hybridization data were processed as described in chapter 6.10 using the Bruker-based macro program. For each combinatorial clone pair (clone x versus clone y), Pearson correlations were calculated. Clones are depicted in their respective cluster (Cl. A, C, D, E) and Pearson correlations of each individual clone are sorted by number. Those clones that belong to the same respective cluster are marked by green color. The clone under investigation is made stand out in black bold type. All clones possess internal tracking codes.



**Figure 7.11 Hybridization results of selected genomic DNA clones hybridized with global PNA sets**

MALDI-TOF mass spectra of each time three unrelated clones are depicted that were hybridized either with PNA set “6mer global” or PNA set “7mer global”. Experimental probe masses are annotated. Compositions of either PNA sets are given in chapter 5.7.

each time, three unrelated clones that were hybridized with either global PNA sets, respectively. It is evident that out of 40 PNA probes applied only a few distinct PNA probes show up. Furthermore, hybridization profiles are very similar rendering discrimination by profile correlation very difficult. Therefore, it can be concluded that, despite the simultaneous detection of 40 PNA hexamer and heptamer probes, a 40-plex hybridization approach does not deliver meaningful hybridization data and hence is impracticable.

Beside the evaluation of global PNA sets, less complex 6mer and 7mer subsets were tested. These comprise sets “6mer sub1” consisting of 21 PNA probes, “6mer sub2” (17 probes), “6mer sub3” (15 probes), “7mer sub1” (20 probes), and “7mer sub2” (20 probes). In general, hybridization performances of these sets were very heterogeneous, i.e. correlation analyses did not reveal the same quality of results. Figure 7.12 shows the correlation data gained for 21 genomic DNA clones of four different clusters and two independent singletons that were hybridized with PNA set “6mer sub1”. 10 clones, including an entire fifth cluster, that did not yield consistent hybridization data



## 7. Results

Cl. A	C22	F21	G08	J06	O21	P22	Cl. C	D11	E14	F13	L11	O12
C22	0,9928	0,9886	0,9941	0,9776	0,9926	0,9776	D11	0,9882	0,9781	0,9873	0,9882	0,9808
P22	0,9638	0,9753	0,9753	0,9719	0,9699	0,9651	L11	0,9561	0,9645	0,9271	0,9645	0,9326
O21	0,9487	0,9718	0,9719	0,9718	0,9662	0,9638	E14	0,9347	0,9347	0,9230	0,9347	0,9315
J06	0,9455	0,9699	0,9688	0,9467	0,9467	0,9467	O12	0,9326	0,9315	0,9148	0,9137	0,9271
F21	0,9442	0,9651	0,9662	0,9455	0,9455	0,9455	F13	0,9230	0,9148	0,9148	0,9122	0,9122
G08	0,9420	0,9442	0,9634	0,9293	0,9345	0,9293	E08	0,8827	0,8812	0,8778	0,9051	0,7913
C03	0,9328	0,9195	0,9467	0,8753	0,8741	0,8770	K04	0,8739	0,8667	0,8622	0,8998	0,8998
A06	0,9099	0,9096	0,9420	0,8737	0,8658	0,8762	A06	0,8593	0,8574	0,8060	0,8875	0,7568
L24	0,8986	0,9044	0,9188	0,8646	0,8557	0,8557	A11	0,8431	0,8522	0,8522	0,8908	0,7811
K04	0,8769	0,8857	0,8998	0,8598	0,8549	0,8790	G08	0,8402	0,8463	0,8463	0,8766	0,7493
K18	0,8754	0,8787	0,8841	0,8646	0,8472	0,8472	K18	0,8311	0,8337	0,8337	0,8732	0,7374
P19	0,8703	0,8770	0,8806	0,8435	0,8216	0,8216	P19	0,8224	0,8284	0,8284	0,8580	0,7364
P06	0,8682	0,8752	0,8772	0,8378	0,8214	0,8214	B03	0,8189	0,8034	0,8034	0,8524	0,7217
E08	0,8495	0,8580	0,8598	0,8271	0,7892	0,7170	F21	0,8082	0,7971	0,7971	0,8448	0,7079
A11	0,8122	0,8550	0,8509	0,8033	0,7859	0,7015	L24	0,7982	0,7844	0,7844	0,8303	0,6982
L11	0,7818	0,8332	0,8463	0,7837	0,7857	0,6970	C03	0,7918	0,7842	0,7842	0,8271	0,6930
D11	0,7508	0,8082	0,8111	0,7824	0,7653	0,6785	P06	0,7886	0,7837	0,7837	0,8058	0,6749
E14	0,7346	0,8034	0,8239	0,7697	0,7145	0,6722	O21	0,7859	0,7790	0,7790	0,7943	0,6705
O12	0,6589	0,6836	0,6836	0,7192	0,7079	0,6310	J06	0,7697	0,7682	0,7682	0,7882	0,6589
F13	0,6568	0,6606	0,6606	0,7001	0,6668	0,6035	C03	0,7508	0,7346	0,7346	0,7833	0,6356
B03	0,6097	0,6356	0,6356	0,6367	0,5979	0,5921	P22	0,7456	0,7145	0,7145	0,7818	0,5888

Cl. B	A06	A11	C03	K04	K18	Cl. D	L24	P06	P19	singl.	B03	singl.	E08
A06	0,9935	0,9892	0,9980	0,9920	0,9977	L24	0,9904	0,9902	0,9905	B03	0,9965	E08	0,9908
K18	0,9892	0,9645	0,9790	0,9702	0,9892	P06	0,9414	0,9738	0,9738	E08	0,8467	A11	0,9458
C03	0,9790	0,9616	0,9506	0,9613	0,9645	P19	0,9402	L24	0,9402	F13	0,8272	A06	0,9333
K04	0,9702	0,9458	0,9362	0,9506	0,9613	G08	0,9188	C03	0,9024	A06	0,8189	K04	0,8968
G08	0,9688	0,9447	0,9328	0,9467	0,9362	A06	0,9094	K18	0,8992	C03	0,8106	C03	0,8934
A11	0,9616	0,9207	0,9207	0,9447	0,8992	F21	0,9044	A06	0,8815	K04	0,7971	L11	0,8908
E08	0,9333	0,8765	0,9040	0,9096	0,8754	C22	0,8986	F21	0,8770	F21	0,8787	A11	0,8827
F21	0,9195	0,8621	0,9024	0,9031	0,8752	K04	0,8964	P22	0,8762	G08	0,8772	K04	0,8812
P19	0,9174	0,8574	0,8934	0,8975	0,8732	E08	0,8995	E08	0,8717	P22	0,8770	O12	0,7568
L11	0,9137	0,8909	0,8857	0,8968	0,8646	C03	0,8673	C22	0,8682	C22	0,8703	L24	0,8778
C22	0,9099	0,8483	0,8841	0,8964	0,8571	A11	0,8621	G08	0,8598	K18	0,8571	A06	0,8717
L24	0,9094	0,8431	0,8673	0,8769	0,8496	O21	0,8549	L11	0,8524	O21	0,8557	G08	0,7192
P06	0,8815	0,8400	0,8598	0,8753	0,8311	K18	0,8496	K04	0,8496	A11	0,8483	P19	0,7181
O21	0,8741	0,8332	0,8448	0,8739	0,8284	J06	0,8378	A06	0,8472	J06	0,8435	P06	0,6953
J06	0,8737	0,8122	0,8434	0,8667	0,8239	L11	0,8058	L11	0,8400	L11	0,8365	K18	0,8467
D11	0,8593	0,8106	0,7918	0,8658	0,8214	D11	0,7982	E14	0,8337	D11	0,8224	C03	0,6842
E14	0,8522	0,8090	0,7844	0,8496	0,8076	E14	0,7682	O21	0,8216	E08	0,8198	P22	0,6785
F13	0,7540	0,7824	0,7824	0,7749	0,7303	F13	0,7352	D11	0,7888	E14	0,7842	F21	0,6908
O12	0,7374	0,7653	0,6930	0,7701	0,6882	B03	0,7315	F13	0,7311	F13	0,7725	J06	0,6367
B03	0,7303	0,7551	0,6842	0,7666	0,6938	O12	0,7217	B03	0,6853	O12	0,7483	C22	0,6097
P22	0,6722	0,7015	0,6021	0,6970	0,5999	P22	0,6310	O12	0,6705	B03	0,7181	O21	0,7857

**Figure 7.12 Correlation analysis of genomic DNA clones hybridized with PNA set “6mer sub1”**

Genomic DNA clones were hybridized with PNA set “6mer sub1”. Hybridization data were processed and Pearson correlations were calculated as described earlier. Clones are depicted in their respective cluster (Cl. A, B, C, D) or as cluster-independent singleton (singl.). Those clones that belong to the same respective cluster are marked by green color. The clone under investigation is made stand out in black bold type. All clones possess internal tracking codes.

were excluded from the analysis. This was done to avoid a subsequent impairment of the overall analysis. The figure demonstrates that - apart from a very few exceptions - related clones of a respective cluster are grouped together and are completely separated from unrelated ones although the numeric difference to those unrelated clones is mostly rather small ( $< \Delta 0,03$ ). For some clones, though, such as O21, P22, or O12, the correlation difference achieved is much higher as is for singletons B03 and E08 ( $\Delta 0,04-0,15$ ). Figure 7.13 exhibits MALDI-TOF mass spectra of six genomic DNA clones that were hybridized with PNA set “6mer sub1”: two clone pairs from two different clusters and two singletons. The figure clearly shows that at least for the clones presented even a visual discrimination would be possible confirming the high performance of PNA set “6mer sub1” in distinguishing clones on the basis of hybridization profiles.

In contrast to PNA set “6mer sub1” hybridization performances of the other two 6mer as well as the 7mer subsets were less satisfactory. Figure 7.14 shows the correlation data gained for 20 genomic DNA clones of four different clusters and two independent

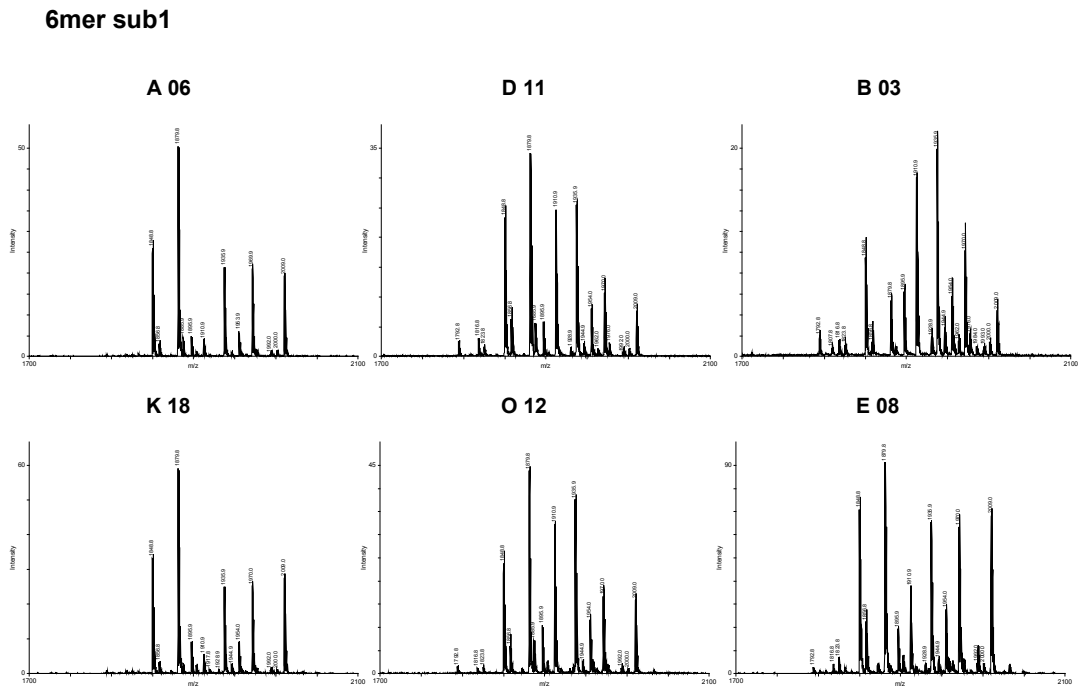


**Figure 7.13 Hybridization results of selected genomic DNA clones hybridized with PNA set “6mer sub1”**

MALDI-TOF mass spectra of six genomic DNA clones are depicted that were hybridized with PNA set “6mer sub1”. A06 and K18 belong to one cluster, D11 and O12 to another one. B03 and E08 are singletons. Experimental probe masses are annotated. The composition of the PNA set is given in chapter 5.7

singletons that were hybridized with PNA set “6mer sub2”. To avoid a subsequent impairment of the overall analysis, 11 clones that did not yield consistent hybridization data were again excluded from the analysis. The figure clearly shows the inferior performance compared to set “6mer sub1”. Related clones of a given cluster are hardly separated from unrelated ones and, if so, numeric correlation differences are negligible. However, for a few clones, such as A11, C03, and singletons B03 and E08, the discrimination achieved is better. Furthermore, a general trend towards correct discrimination is still discernible. As for the remaining PNA sets, set “6mer sub3” and “7mer sub1” yielded correlation data of comparable modest quality whereas PNA set “7mer sub2” failed to generate consistent data at all.

### 7.3.2 Analysis of cDNA clones

21 sequence-confirmed cDNA clones, that are void of repeat regions, were analyzed by hybridization to prevent artifacts and hence additional sources of experimental error.

## 7. Results

Cl. A	C22	F21	F21	H14	J20	O21	Cl. B	A11	C03	K04	K18	singl.	B03		
C22	<b>0,9927</b>	F21	<b>0,9968</b>	F21	<b>0,9865</b>	J20	<b>0,9895</b>	A11	<b>0,9910</b>	C03	<b>0,9702</b>	K04	<b>0,9938</b>	B03	<b>0,9350</b>
F21	<b>0,9893</b>	M10	<b>0,9895</b>	H14	<b>0,9839</b>	F21	<b>0,9819</b>	C22	<b>0,9877</b>	K18	<b>0,9872</b>	K04	<b>0,9872</b>	D11	<b>0,8695</b>
O21	<b>0,9877</b>	C22	<b>0,9893</b>	M10	<b>0,9834</b>	K04	<b>0,9794</b>	F21	<b>0,9837</b>	K04	<b>0,9727</b>	A11	<b>0,9580</b>	E08	<b>0,8434</b>
M10	<b>0,9817</b>	J19	<b>0,9866</b>	J19	<b>0,9818</b>	C22	<b>0,9726</b>	H14	<b>0,9748</b>	C03	<b>0,9580</b>	K18	<b>0,9488</b>	L11	<b>0,8348</b>
H14	<b>0,9804</b>	H14	<b>0,9865</b>	C22	<b>0,9804</b>	H14	<b>0,9705</b>	M10	<b>0,9744</b>	J20	<b>0,9464</b>	J20	<b>0,9104</b>	C14	<b>0,8320</b>
J19	<b>0,9763</b>	O21	<b>0,9837</b>	C14	<b>0,9775</b>	M10	<b>0,9694</b>	J20	<b>0,9667</b>	F21	<b>0,9159</b>	F21	<b>0,8687</b>	H07	<b>0,8291</b>
C14	<b>0,9731</b>	J20	<b>0,9819</b>	O21	<b>0,9748</b>	K18	<b>0,9668</b>	J19	<b>0,9648</b>	C22	<b>0,9076</b>	O21	<b>0,8616</b>	J20	<b>0,8291</b>
L11	<b>0,9663</b>	H07	<b>0,9714</b>	L11	<b>0,9692</b>	O21	<b>0,9667</b>	L11	<b>0,9578</b>	H14	<b>0,8995</b>	H14	<b>0,8451</b>	P06	<b>0,8223</b>
H07	<b>0,9598</b>	O12	<b>0,9702</b>	H07	<b>0,9689</b>	C14	<b>0,9622</b>	K04	<b>0,9543</b>	M10	<b>0,8942</b>	M10	<b>0,8383</b>	J19	<b>0,8270</b>
K04	<b>0,9587</b>	L11	<b>0,9679</b>	O12	<b>0,9686</b>	H07	<b>0,9593</b>	H07	<b>0,9482</b>	J19	<b>0,8870</b>	C14	<b>0,8301</b>	O21	<b>0,8213</b>
O12	<b>0,9587</b>	K04	<b>0,9662</b>	K04	<b>0,9535</b>	O12	<b>0,9526</b>	O12	<b>0,9454</b>	H07	<b>0,8819</b>	H07	<b>0,8214</b>	H07	<b>0,8227</b>
N21	<b>0,9428</b>	D11	<b>0,9496</b>	N21	<b>0,9519</b>	A11	<b>0,9464</b>	N21	<b>0,9306</b>	C14	<b>0,8816</b>	J19	<b>0,8184</b>	C14	<b>0,9187</b>
K18	<b>0,9306</b>	N21	<b>0,9489</b>	D11	<b>0,9498</b>	D11	<b>0,9356</b>	K18	<b>0,9237</b>	O12	<b>0,8709</b>	E08	<b>0,8090</b>	O12	<b>0,9126</b>
D11	<b>0,9299</b>	K18	<b>0,9435</b>	P06	<b>0,9321</b>	L11	<b>0,9287</b>	D11	<b>0,9128</b>	E08	<b>0,8639</b>	O12	<b>0,8010</b>	D11	<b>0,9042</b>
P06	<b>0,9143</b>	P06	<b>0,9265</b>	K18	<b>0,9280</b>	C03	<b>0,9104</b>	A11	<b>0,9066</b>	D11	<b>0,8394</b>	P06	<b>0,7886</b>	L11	<b>0,8960</b>
A11	<b>0,9076</b>	A11	<b>0,9159</b>	A11	<b>0,8995</b>	N21	<b>0,9099</b>	P06	<b>0,8997</b>	L11	<b>0,8123</b>	D11	<b>0,7811</b>	E08	<b>0,8952</b>
C03	<b>0,8537</b>	E08	<b>0,8693</b>	E08	<b>0,8625</b>	E08	<b>0,8977</b>	C03	<b>0,8616</b>	N21	<b>0,7806</b>	N21	<b>0,7716</b>	N21	<b>0,8348</b>
E08	<b>0,8337</b>	C03	<b>0,8687</b>	C03	<b>0,8451</b>	P06	<b>0,8769</b>	E08	<b>0,8116</b>	B03	<b>0,7752</b>	L11	<b>0,7576</b>	P06	<b>0,8347</b>
B03	<b>0,8016</b>	B03	<b>0,8101</b>	B03	<b>0,8117</b>	B03	<b>0,8291</b>	B03	<b>0,8048</b>	P06	<b>0,7351</b>	B03	<b>0,7311</b>	B03	<b>0,7938</b>

Cl. C	D11	L11	N21	O12	Cl. E	C14	H07	J19	M10	singl.	E08				
D11	<b>0,9897</b>	L11	<b>0,9993</b>	N21	<b>0,9939</b>	J19	<b>0,9884</b>	J19	<b>0,9869</b>	J19	<b>0,9860</b>	J19	<b>0,9919</b>	E08	<b>0,9908</b>
O12	<b>0,9743</b>	N21	<b>0,9901</b>	L11	<b>0,9901</b>	O12	<b>0,9870</b>	M10	<b>0,9835</b>	H07	<b>0,9820</b>	M10	<b>0,9915</b>	D11	<b>0,9209</b>
J19	<b>0,9731</b>	P06	<b>0,9819</b>	P06	<b>0,9869</b>	M10	<b>0,9787</b>	C14	<b>0,9829</b>	O12	<b>0,9783</b>	O12	<b>0,9884</b>	F21	<b>0,9895</b>
N21	<b>0,9667</b>	J19	<b>0,9801</b>	J19	<b>0,9727</b>	H07	<b>0,9783</b>	F21	<b>0,9808</b>	M10	<b>0,9779</b>	C14	<b>0,9869</b>	C14	<b>0,9835</b>
H07	<b>0,9656</b>	M10	<b>0,9769</b>	O12	<b>0,9669</b>	C14	<b>0,9778</b>	F21	<b>0,9778</b>	F21	<b>0,9752</b>	F21	<b>0,9866</b>	H14	<b>0,9834</b>
C14	<b>0,9638</b>	C14	<b>0,9756</b>	D11	<b>0,9667</b>	D11	<b>0,9743</b>	H14	<b>0,9775</b>	F21	<b>0,9714</b>	H07	<b>0,9860</b>	C22	<b>0,9817</b>
M10	<b>0,9592</b>	O12	<b>0,9715</b>	C14	<b>0,9653</b>	L11	<b>0,9715</b>	L11	<b>0,9756</b>	H14	<b>0,9689</b>	H14	<b>0,9818</b>	O12	<b>0,9787</b>
P06	<b>0,9590</b>	H14	<b>0,9692</b>	M10	<b>0,9632</b>	F21	<b>0,9702</b>	H07	<b>0,9752</b>	D11	<b>0,9656</b>	L11	<b>0,9801</b>	H07	<b>0,9779</b>
L11	<b>0,9583</b>	F21	<b>0,9679</b>	H07	<b>0,9567</b>	H14	<b>0,9686</b>	C22	<b>0,9731</b>	L11	<b>0,9636</b>	C22	<b>0,9763</b>	L11	<b>0,9769</b>
H14	<b>0,9498</b>	C22	<b>0,9663</b>	H14	<b>0,9519</b>	N21	<b>0,9669</b>	N21	<b>0,9653</b>	C22	<b>0,9598</b>	D11	<b>0,9731</b>	O21	<b>0,9744</b>
F21	<b>0,9496</b>	H07	<b>0,9636</b>	F21	<b>0,9489</b>	C22	<b>0,9587</b>	O21	<b>0,9648</b>	J20	<b>0,9593</b>	N21	<b>0,9727</b>	J20	<b>0,9694</b>
J20	<b>0,9356</b>	D11	<b>0,9583</b>	C22	<b>0,9428</b>	P06	<b>0,9559</b>	D11	<b>0,9638</b>	N21	<b>0,9567</b>	J20	<b>0,9667</b>	N21	<b>0,9632</b>
C22	<b>0,9299</b>	O21	<b>0,9578</b>	O21	<b>0,9306</b>	J20	<b>0,9526</b>	J20	<b>0,9622</b>	O21	<b>0,9482</b>	O21	<b>0,9648</b>	D11	<b>0,9592</b>
E08	<b>0,9209</b>	J20	<b>0,9287</b>	J20	<b>0,9099</b>	O21	<b>0,9454</b>	P06	<b>0,9503</b>	K04	<b>0,9441</b>	P06	<b>0,9582</b>	K04	<b>0,9538</b>
O21	<b>0,9128</b>	K04	<b>0,8960</b>	K04	<b>0,8743</b>	K04	<b>0,9367</b>	K04	<b>0,9416</b>	P06	<b>0,9416</b>	K04	<b>0,9515</b>	P06	<b>0,9455</b>
K04	<b>0,9042</b>	K18	<b>0,8558</b>	E08	<b>0,8368</b>	K18	<b>0,9126</b>	K18	<b>0,9187</b>	K18	<b>0,9227</b>	K18	<b>0,9270</b>	K18	<b>0,9289</b>
K18	<b>0,8847</b>	B03	<b>0,8348</b>	K18	<b>0,8348</b>	E08	<b>0,9028</b>	A11	<b>0,8816</b>	E08	<b>0,8982</b>	E08	<b>0,8957</b>	A11	<b>0,8942</b>
B03	<b>0,8695</b>	E08	<b>0,8187</b>	B03	<b>0,8254</b>	A11	<b>0,8709</b>	E08	<b>0,8774</b>	A11	<b>0,8819</b>	A11	<b>0,8870</b>	E08	<b>0,8720</b>
A11	<b>0,8394</b>	A11	<b>0,8123</b>	A11	<b>0,7806</b>	B03	<b>0,8213</b>	B03	<b>0,8320</b>	B03	<b>0,8291</b>	B03	<b>0,8216</b>	C03	<b>0,8383</b>
C03	<b>0,7811</b>	C03	<b>0,7576</b>	C03	<b>0,7716</b>	C03	<b>0,8010</b>	C03	<b>0,8301</b>	C03	<b>0,8214</b>	C03	<b>0,8184</b>	B03	<b>0,8170</b>

**Figure 7.14 Correlation analysis of genomic DNA clones hybridized with PNA set “6mer sub2”**

Genomic DNA clones were hybridized with PNA set “6mer sub2”. Hybridization data were processed and Pearson correlations were calculated as described earlier. Clones are depicted in their respective cluster (Cl. A, B, C, E) or as cluster-independent singleton (singl.). Those clones that belong to the same respective cluster are marked by green color. The clone under investigation is made stand out in black bold type. All clones possess internal tracking codes.

These 21 clones fall into five clusters of different size. In addition, 8 shorter PCR fragments of four of these clones were generated to yield a total of 29 clones to be analyzed. Analogous to genomic DNA clones, all clones were hybridized with the available PNA 6mer and 7mer subsets which, in turn, revealed very heterogeneous hybridization performances. Figure 7.15 shows the correlation data gained for 23 cDNA clones of five different clusters that were hybridized with PNA set “6mer sub1”. 6 clones that did not yield consistent hybridization results were excluded from the analysis to avoid a subsequent impairment of the overall analysis. The figure clearly shows that –as for genomic DNA clones and apart from a very few exceptions - related clones of a respective cluster are grouped together and are completely separated from unrelated ones. Numeric differences to unrelated clones are mostly rather small though ( $< \Delta 0,03$ ). For some clones, however, such as H182, I151, or K022, the correlation difference achieved is much higher ( $\Delta 0,06-0,12$ ). As in the case of genomic DNA clones, the high performance of PNA set “6mer sub1” in distinguishing clones was also confirmed by original spectra.

## 7. Results

Cl. 1	H109	H182	H182a	H182b	H151	P156	Cl. 5	B112	C017	F231	F231	N158	P091	P091
H109	0.9918	H182b	0.9765	H182a	0.9953	H182b	0.9927	H1151	0.9713	P156	0.9732	H1151	0.9732	H1151
P156	0.9732	H182	0.9727	H182b	0.9716	H182	0.9765	P156	0.9489	H109	0.9732	F231	0.9727	F231
H182	0.9430	H182a	0.9562	H182	0.9716	H109	0.9430	H151	0.9489	H109	0.9430	H1151	0.9727	H1151
H182	0.9274	P156	0.9299	P156	0.9241	P156	0.9295	H182	0.9291	H182	0.9299	N158	0.9685	B112
H182a	0.9222	H151	0.9291	H109	0.9222	H109	0.9213	H182b	0.9005	H182b	0.9295	P091	0.9675	C017
H182b	0.9213	H109	0.9274	A071a	0.9187	A071a	0.9101	H182a	0.8992	H182a	0.9241	K022b	0.9451	N178
A071	0.8848	A071b	0.8061	K022a	0.9006	I051	0.9021	N158	0.8094	P091	0.9117	I051	0.9379	H035
F231	0.8722	A071a	0.8015	I051	0.8994	K022b	0.9008	A071a	0.7880	N158	0.9090	A071a	0.9315	A071a
N158	0.8602	N178	0.7851	H151	0.8992	H151	0.9005	P091	0.7718	F231	0.9032	H035	0.9232	I051
A071b	0.8598	H035	0.7664	K022b	0.8909	K022a	0.9002	M098	0.7638	C017	0.8901	K022a	0.9219	K022b
H035	0.8576	A071	0.7445	B112	0.8878	H035	0.8885	I051	0.7635	B112	0.8897	D178	0.9146	A071b
C017	0.8540	M098	0.7274	N158	0.8838	B112	0.8883	N178	0.7570	H035	0.8860	M098	0.9102	M098
B112	0.8450	I051	0.7259	N063	0.8831	F231	0.8832	H035	0.7502	A071a	0.8807	N178	0.9096	D178
P091	0.8425	N158	0.7229	H035	0.8771	N063	0.8780	K022a	0.7433	K022b	0.8806	N063	0.8967	A071
A071a	0.8362	K022	0.7079	F231	0.8748	N158	0.8775	K022	0.7424	D178	0.8766	A071	0.8944	K022a
M098	0.8336	P091	0.7053	C017	0.8726	N178	0.8743	B112	0.7313	K022a	0.8764	P156	0.8897	N063
K022b	0.8332	B112	0.7006	M098	0.8701	C017	0.8692	A071b	0.7211	I051	0.8729	H182b	0.8883	P156
D178	0.8216	K022a	0.6771	D178	0.8671	K022	0.8650	F231	0.6824	M098	0.8648	H182a	0.8878	H182a
K022a	0.8184	D178	0.6670	N178	0.8591	M098	0.8576	C017	0.6761	N063	0.8540	A071b	0.8815	H182a
N178	0.8149	C017	0.6651	A071b	0.8567	D178	0.8572	K022b	0.6755	A071	0.8537	H109	0.8450	H109
N063	0.7799	F231	0.6574	K022	0.8529	P091	0.8550	A071	0.6563	N178	0.8533	K022	0.7734	K022
I051	0.7740	N063	0.6519	P091	0.8429	A071b	0.8318	D178	0.6469	A071b	0.8383	H151	0.7313	I151
K022	0.7245	K022b	0.6519	A071	0.8418	N063	0.8075	N063	0.6304	K022	0.7781	H182	0.7079	H182
A071	0.9903	A071a	0.9926	A071b	0.9903	M098	0.9796	K022	0.9777	K022a	0.9810	K022b	0.9890	N178
A071b	0.9785	M098	0.9717	A071	0.9785	A071a	0.9717	K022a	0.9424	K022b	0.9523	K022a	0.9523	C017
A071a	0.9526	A071	0.9526	A071a	0.9512	A071	0.9481	K022b	0.9352	K022	0.9424	B112	0.9451	K022b
M098	0.9481	A071b	0.9512	M098	0.9480	A071b	0.9480	N178	0.9277	N178	0.9397	N178	0.9426	K022a
C017	0.9123	I051	0.9457	C017	0.9177	C017	0.9157	H182b	0.8650	I051	0.9338	F231	0.9419	F231
F231	0.9122	C017	0.9453	F231	0.9134	B112	0.9102	H182a	0.8529	N063	0.9295	K022	0.9352	A071a
H035	0.8981	F231	0.9393	H035	0.8957	F231	0.9058	A071a	0.8480	A071a	0.9242	C017	0.9214	K022
B112	0.8944	N178	0.9317	N178	0.8826	I051	0.8811	I051	0.8388	H035	0.9235	N158	0.9151	B112
H109	0.8849	B112	0.9315	B112	0.8815	N178	0.8783	N158	0.8252	B112	0.9219	N063	0.9120	H035
N178	0.8828	K022a	0.9242	K022b	0.8804	K022b	0.8771	H035	0.8105	N158	0.9171	D178	0.9120	I051
K022b	0.8794	H182a	0.9187	D178	0.8729	N158	0.8703	P091	0.7963	F231	0.9133	A071a	0.9109	P091
D178	0.8692	H035	0.9166	K022a	0.8675	P091	0.8702	M098	0.7914	D178	0.9103	I051	0.9097	A071
K022a	0.8653	N158	0.9115	I051	0.8633	H182a	0.8701	P156	0.7781	C017	0.9039	H035	0.9033	A071b
P156	0.8537	K022b	0.9109	H109	0.8588	H035	0.8692	B112	0.7734	H182a	0.9006	H182b	0.9008	M098
P091	0.8501	H182b	0.9101	N158	0.8570	P156	0.8648	F231	0.7649	H182b	0.9002	P091	0.8788	H182a
I051	0.8488	P091	0.8890	H182a	0.8567	K022a	0.8631	A071b	0.7638	P091	0.8788	H182a	0.8909	N158
N063	0.8434	N063	0.8818	N063	0.8486	H182b	0.8576	H151	0.7424	P156	0.8764	P156	0.8806	N063
N158	0.8428	P156	0.8807	P156	0.8383	N063	0.8515	N063	0.7331	A071b	0.8675	A071b	0.8804	D178
H182a	0.8418	D178	0.8767	H182b	0.8318	D178	0.8416	A071	0.7303	A071	0.8853	A071	0.8794	H182a
H182b	0.8075	K022	0.8480	P091	0.8308	H109	0.8336	H109	0.7245	M098	0.8831	M098	0.8771	P156
H182	0.7445	H109	0.8362	H182	0.8061	K022	0.7914	C017	0.7204	H098	0.8184	H109	0.8332	H109
K022	0.7303	H182	0.8015	K022	0.7638	H151	0.7638	D178	0.7203	I151	0.7433	H151	0.6755	H182
I151	0.6563	I151	0.7880	I151	0.7211	H182	0.7274	H182	0.7079	H182	0.6771	H182	0.6393	I151
D178	0.9953	H035	0.9672	D178	0.9672	N063	0.9794	I051	0.9929	N063	0.9929	D178	0.9602	D178
H035	0.9672	D178	0.9672	N063	0.9794	I051	0.9794	I051	0.9602	D178	0.9602	D178	0.9602	D178
N063	0.9641	N063	0.9618	D178	0.9602	D178	0.9618	H035	0.9597	H035	0.9618	H035	0.9597	H035
I051	0.9602	I051	0.9587	H035	0.9597	H035	0.9618	F231	0.9201	F231	0.9466	A071a	0.9457	K022a
F231	0.9201	F231	0.9466	A071a	0.9457	K022a	0.9295	F231	0.9123	I051	0.9338	F231	0.9419	F231
C017	0.9147	C017	0.9454	B112	0.9378	K022b	0.9120	C017	0.9147	C017	0.9454	B112	0.9378	K022b
B112	0.9146	K022a	0.9235	N158	0.9341	N158	0.9077	B112	0.9146	K022a	0.9235	N158	0.9341	N158
K022a	0.9133	B112	0.9232	K022a	0.9338	B112	0.8957	K022a	0.9133	B112	0.9232	K022a	0.9338	B112
K022b	0.9120	A071a	0.9166	C017	0.9248	C017	0.9248	C017	0.9120	A071a	0.9166	C017	0.9248	C017
P091	0.8877	N158	0.9079	F231	0.9190	F231	0.8922	P091	0.8877	N158	0.9079	F231	0.9190	F231
N158	0.8809	K022b	0.9033	K022b	0.9097	H182a	0.8831	N158	0.8809	K022b	0.9033	K022b	0.9097	H182a
A071a	0.8767	N178	0.8982	H182b	0.9021	A071a	0.8818	A071a	0.8767	N178	0.8982	H182b	0.9021	A071a
P156	0.8766	A071	0.8981	H182a	0.8994	H182b	0.8780	P156	0.8766	A071	0.8981	H182a	0.8994	H182b
A071b	0.8729	A071b	0.8957	P091	0.8935	P091	0.8771	A071b	0.8729	A071b	0.8957	P091	0.8935	P091
A071	0.8692	H182b	0.8885	N178	0.8925	N178	0.8632	A071	0.8692	H182b	0.8885	N178	0.8925	N178
H182a	0.8671	P156	0.8860	M098	0.8811	P156	0.8540	H182a	0.8671	P156	0.8860	M098	0.8811	P156
N178	0.8596	P091	0.8834	P156	0.8729	M098	0.8510	N178	0.8596	P091	0.8834	P156	0.8729	M098
H182b	0.8572	H182a	0.8771	A071b	0.8486	A071b	0.8486	H182b	0.8572	H182a	0.8771	A071b	0.8486	A071b
M098	0.8416	M098	0.8632	A071	0.8434	A071	0.8434	M098	0.8416	M098	0.8632	A071	0.8434	A071
H109	0.8216	H109	0.8576	K022	0.8388	H109	0.7799	H109	0.8216	H109	0.8576	K022	0.8388	H109
K022	0.7203	K022	0.8105	H109	0.7740	K022	0.7331	H182	0.6670	H182	0.7664	H151	0.7635	H182
H182	0.6670	H182	0.7664	H151	0.7635	H182	0.6519	H182	0.6469	H151	0.7502	H182	0.7259	H151

**Figure 7.15 Correlation analysis of cDNA clones hybridized with PNA set “6mer sub1”**

cDNA clones were hybridized with PNA set “6mer sub1”. Hybridization data were processed and Pearson correlations were calculated as described earlier. Clones are depicted in their respective cluster (Cl. 1, 2, 3, 4, 5). Those clones that belong to the same respective cluster are marked by green color. The clone under investigation is made stand out in black bold type. All clones possess internal tracking codes. Shorter PCR fragments of original clones are indicated by codes with lower case letters “a” and “b”.

Figure 7.16 exhibits MALDI-TOF mass spectra of six cDNA clones that were hybridized with PNA set “6mer sub1”: three clone pairs from three different clusters. The figure visually supports the successful clone discrimination.

Similar to genomic DNA clones, the other two 6mer as well as the 7mer subsets performed worse. Figure 7.17 shows the correlation data gained for 17 cDNA clones of four different clusters that were hybridized with PNA set “6mer sub2”. To avoid a subsequent impairment of the overall analysis, 12 clones, including an entire fifth cluster, that did not yield consistent hybridization results were excluded from the analysis. The figure clearly demonstrates the inferior performance compared to set “6mer sub1”. Related clones of a given cluster are again hardly separated from unrelated ones and numeric correlation differences are negligible. Although a general trend towards correct discrimination is still somewhat discernible, for the cDNA clones tested the discrimination performance of PNA set “6mer sub2” was even worse compared to genomic DNA clones.

## 7. Results

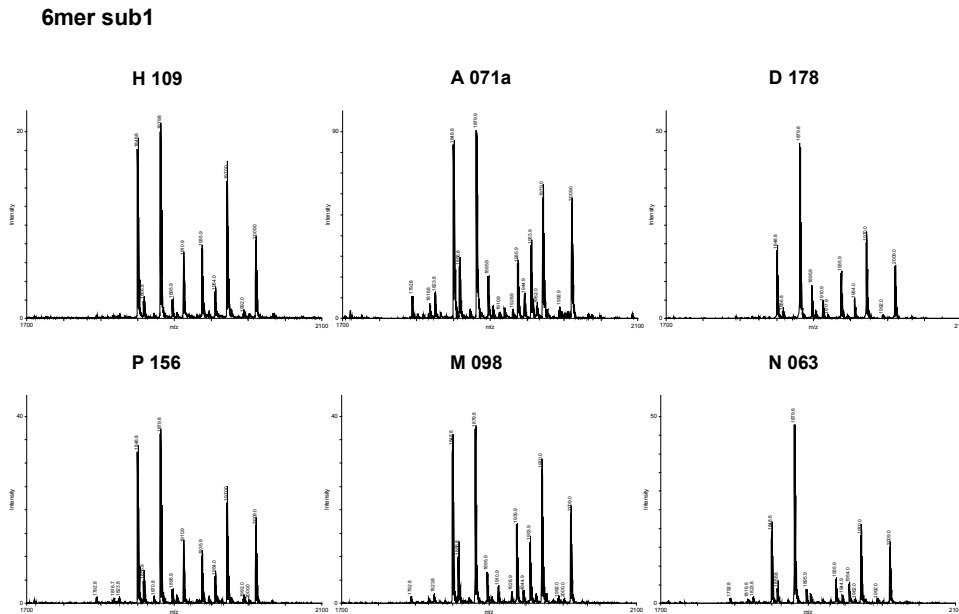


**Figure 7.16 Hybridization results of selected cDNA clones hybridized with PNA set “6mer sub1”**

MALDI-TOF mass spectra of six cDNA clones are depicted that were hybridized with PNA set “6mer sub1”. H109 and P156 belong to one cluster, A071a and M098 to another one, D178 and N063 to a third cluster. Experimental probe masses are annotated. The composition of the PNA set is given in chapter 5.7.

Cl. 1	B219	H109	H182	H151	P156	Cl. 3	E033	G173	K022	K022a
P156	0,9879	H109 0,9948	H182 0,9960	H151 0,9951	P156 0,9991	K022a	0,9754	G173 0,9961	K022 0,9932	K022a 0,9955
H109	0,9854	B219 0,9854	H109 0,9853	P156 0,9892	H035 0,9900	E033	0,9740	K022 0,9791	G173 0,9791	H182 0,9814
B219	0,9843	H182 0,9853	K022a 0,9814	P091 0,9853	H151 0,9892	H182	0,9675	K022a 0,9776	K022a 0,9755	H109 0,9813
H182	0,9787	K022a 0,9813	B219 0,9787	H035 0,9836	B219 0,9879	H109	0,9672	H109 0,9680	P156 0,9721	G173 0,9776
H151	0,9770	H151 0,9738	P156 0,9719	D178 0,9822	N158 0,9871	G173	0,9664	B219 0,9672	H109 0,9718	B219 0,9759
K022a	0,9759	K022 0,9718	E033 0,9675	N063 0,9772	L028 0,9856	B219	0,9651	E033 0,9664	D178 0,9647	K022 0,9755
G173	0,9672	G173 0,9680	H151 0,9658	B219 0,9770	P091 0,9847	K022	0,9422	H182 0,9510	H182 0,9607	E033 0,9754
E033	0,9651	P156 0,9673	P091 0,9632	N158 0,9748	N063 0,9796	H151	0,9253	H151 0,9228	H035 0,9600	I051 0,9579
K022	0,9596	E033 0,9672	K022 0,9607	L028 0,9743	I051 0,9747	P156	0,9238	P156 0,9045	B219 0,9596	P156 0,9543
P091	0,9500	P091 0,9631	B112 0,9545	B112 0,9739	D178 0,9744	P091	0,9076	P091 0,8999	P091 0,9571	P091 0,9379
B112	0,9440	D178 0,9567	G173 0,9510	H109 0,9738	K022 0,9721	B112	0,9001	B112 0,8938	I051 0,9547	B112 0,9273
D178	0,9337	D178 0,9501	H035 0,9439	H182 0,9658	H182 0,9719	D178	0,8875	D178 0,8936	N063 0,9546	H035 0,9238
H035	0,9259	H035 0,9430	N158 0,9339	I051 0,9594	B112 0,9710	H035	0,8852	H035 0,8719	L028 0,9465	D178 0,9230
N158	0,9093	N158 0,9284	D178 0,9324	K022a 0,9579	H109 0,9673	N158	0,8886	N063 0,8563	B112 0,9449	N158 0,9071
N063	0,9089	N063 0,9270	L028 0,9253	K022 0,9547	K022a 0,9543	N063	0,8630	N158 0,8443	N158 0,9442	N063 0,9071
L028	0,9014	L028 0,9220	N063 0,9229	E033 0,9253	E033 0,9238	L028	0,8597	L028 0,8393	E033 0,9422	L028 0,9023
I051	0,8760	I051 0,8977	I051 0,9064	G173 0,9228	G173 0,9045	I051	0,8318	I051 0,8036	I051 0,9238	I051 0,8769

Cl. 4	D178	H035	I051	I051	L028	L028	N063	Cl. 5	B112	N158	P091	P091
D178	0,9937	H035 0,9979	I051 0,9971	L028 0,9953	N158 0,9965	N063 0,9944	0,9981	N158	0,9895	N158 0,9969	P091 0,9979	0,9979
N063	0,9859	L028 0,9949	L028 0,9953	N158 0,9928	I051 0,9953	L028 0,9935	0,9944	P091	0,9869	L028 0,9965	H035 0,9859	0,9869
H035	0,9831	N063 0,9944	N158 0,9928	I051 0,9953	L028 0,9935	0,9935	0,9944	B112	0,9865	H035 0,9943	H035 0,9858	0,9858
I151	0,9822	N158 0,9943	H035 0,9875	H035 0,9949	N158 0,9900	0,9900	0,9900	I151	0,9739	I051 0,9928	N158 0,9854	0,9854
P091	0,9759	P156 0,9900	N063 0,9857	N063 0,9935	D178 0,9859	0,9859	0,9859	H035	0,9732	N063 0,9900	I151 0,9853	0,9853
L028	0,9756	I051 0,9875	P156 0,9747	P156 0,9856	I051 0,9857	0,9857	0,9857	P156	0,9710	B112 0,9895	P156 0,9847	0,9847
P156	0,9744	P091 0,9858	P091 0,9845	D178 0,9756	P156 0,9796	0,9796	0,9796	D178	0,9697	P156 0,9871	N063 0,9767	0,9767
N158	0,9733	I151 0,9836	D178 0,9597	P091 0,9744	I151 0,9772	0,9772	0,9772	N063	0,9659	P091 0,9854	D178 0,9759	0,9759
B112	0,9697	D178 0,9831	I151 0,9594	I151 0,9743	P091 0,9767	0,9767	0,9767	L028	0,9602	I151 0,9748	L028 0,9744	0,9744
K022	0,9647	B112 0,9732	B112 0,9479	B112 0,9602	B112 0,9659	0,9659	0,9659	H109	0,9567	D178 0,9733	I051 0,9645	0,9645
I051	0,9597	K022 0,9600	K022 0,9238	K022 0,9465	K022 0,9546	0,9546	0,9546	H182	0,9545	K022 0,9442	H182 0,9632	0,9632
H109	0,9501	H182 0,9439	H182 0,9064	H182 0,9253	H109 0,9270	0,9270	0,9270	I051	0,9479	H182 0,9339	H109 0,9631	0,9631
B219	0,9337	H109 0,9430	H109 0,8977	H109 0,9220	H182 0,9229	0,9229	0,9229	B219	0,9449	H109 0,9284	K022 0,9571	0,9571
H182	0,9324	B219 0,9259	K022a 0,8769	K022a 0,9023	B219 0,9089	0,9089	0,9089	B219	0,9440	B219 0,9093	B219 0,9500	0,9500
K022a	0,9230	K022a 0,9238	B219 0,8760	B219 0,9014	K022a 0,9071	0,9071	0,9071	K022a	0,9273	K022a 0,9071	K022a 0,9379	0,9379
G173	0,8936	E033 0,8852	E033 0,8318	E033 0,8597	E033 0,8630	0,8630	0,8630	E033	0,9001	E033 0,8686	E033 0,9076	0,9076
E033	0,8875	G173 0,8719	G173 0,8036	G173 0,8393	G173 0,8563	0,8563	0,8563	G173	0,8938	G173 0,8443	G173 0,8999	0,8999

**Figure 7.17 Correlation analysis of cDNA clones hybridized with PNA set “6mer sub2”**

cDNA clones were hybridized with PNA set “6mer sub2”. Hybridization data were processed and Pearson correlations were calculated as described earlier. Clones are depicted in their respective cluster (Cl. 1, 3, 4, 5). Those clones that belong to the same respective cluster are marked by green color. The clone under investigation is made stand out in black bold type. All clones possess internal tracking codes. Shorter PCR fragments of original clones are indicated by codes with lower case letters “a” and “b”.

Correlation data yielded with the remaining sets were as random as they were for global PNA sets (“6mer sub3” and “7mer sub1”) or failed to generate consistent data at all (“7mer sub2”).

### **7.4 Evaluation of potential DNA immobilization systems for direct hybridization read-out by MALDI-TOF MS**

For full automation and acceleration of the OFP process, a platform would be essential that allows on-site DNA immobilization, probe hybridization and read-out of hybridization events by MALDI-TOF MS. At the beginning of this thesis such a system did not exist - neither in the academic scientific community nor commercially.

Available detection platforms (so-called MALDI targets) normally consist of conductive surfaces (metal, silicon etc.) onto which MALDI matrix and samples are transferred. Optionally, these surfaces can be preloaded with optimized MALDI matrix formulations as in the case of Sequenom’s SpectroCHIP™<sup>12</sup>. In either case, neither immobilization nor hybridization is performed on the surface rendering such a platform unsuitable for the concept of multiplexed OFP. As a consequence, in the scope of the present dissertation it was aimed at the development of a DNA microarray that is compatible with MALDI-TOF MS and suitable for multiplexed OFP.

The majority of conventional DNA microarrays are based on glass slides of 75 mm x 25 mm x 1 mm dimension. This format is used as a universal standard for almost all academically and commercially available microarray chips. To boost the development of a MALDI-TOF MS compatible DNA microarray and to enhance industrial cooperations, a prototype adapter was designed and fabricated that functions as an interface between Bruker MALDI-TOF mass spectrometers and potential DNA chips of universal glass slide format. The adapter was subsequently optimized and possesses the advantage of a flexible design that allows to mount potential chips of roughly the above mentioned dimensions. This flexibility is particularly advantageous for the evaluation of multiple DNA immobilization systems since an individual re-adjustment step for either microarray under investigation or adapter would be practically and economically unfeasible.

---

<sup>12</sup> <http://www.sequenom.com>

### **7.4.1 Promising surfaces and attachment chemistries**

A MALDI-TOF MS compatible DNA immobilization system should feature a high DNA immobilization capacity, a stable attachment chemistry on a solvent resistant conductive surface and a high accessibility of immobilized DNA to hybridization probes and laser desorption. Therefore, in the scope of this dissertation various surfaces and attachment chemistries were evaluated that were likely to fulfill the above mentioned requirements.

#### **7.4.1.1 Acrylamide-based immobilization system**

The immobilization of DNA via a polymeric three-dimensional matrix is supposed to offer a higher immobilization capacity compared to two-dimensional systems. Additionally, no hybridization probe and/or DNA interferences which impair hybridization and its specificity are expected to occur.

Polyacrylamide embodies such a three-dimensional matrix. Two main strategies of immobilizing DNA within such a gel matrix have been proposed. The first is based on an activation of the gel matrix by a reducing agent, mostly hydrazide. Subsequently, modified DNA can be covalently bound to the gel matrix (Khrapko et al., 1991, Yershov et al., 1996). The second strategy focuses on the immobilization of acrylamide-modified oligonucleotides or PCR products by co-polymerization (Rehman et al., 1999). DNA bearing 5'-terminal acrylamide modifications was shown to efficiently co-polymerize with acrylamide monomers to form thermally stable DNA-containing polyacrylamide co-polymers.

Since the activation of gel matrices by strong reducing agents is cumbersome, time-consuming and hazardous, it was decided to concentrate on the co-polymerization strategy. Besides, acrylamide modified PCR products needed for co-polymerization can be readily generated via PCR, employing 5'-acrylamide modified primers which are commercially available. Preliminary experiments on an acrylic silane functionalized MALDI target covered with DNA-containing acrylamide co-polymers showed that - in principle - it is possible to hybridize and detect PNA probes on such a surface. However, several reasons led to the cessation of that approach. First, the co-polymerized gel matrix needs to be completely dried prior to vacuum applied during MALDI-TOF MS measurements. Unfortunately, dried gel matrix on functionalized metal is very unstable and disintegrates. Second, acrylic silane needed for stable functionalization of MALDI targets or other metal surfaces is commercially not available, a custom synthesis would be astronomically expensive. Third, an industrial cooperation giving access to either acrylic silane coated

metal slides or completely functional acrylamide DNA microarrays could not be established. Last, the polymerization mix is very toxic and the time point of polymerization difficult to control. Although polymerization by photo-initiation instead of radical initiation has been successfully employed (Lyubimova et al., 1993), avoiding some of the above mentioned problems, still the required instrumental setup is very costly.

### 7.4.1.2 Streptavidin-based immobilization system

Another promising three-dimensional matrix is a streptavidin-based immobilization system based on self-assembling monolayers (SAM) of long-chain thiol alkanes adsorbed onto a gold layer. Biotin is coupled covalently to the surface and saturated with streptavidin to form an interface for the binding of biotinylated DNA. This system overcomes the length limitation of thiolated DNAs directly coupled to a pure gold layer (Steel et al., 2000) since it combines the robustness of a gold-based SAM immobilization scheme with the high accessibility of streptavidin bound biotinylated DNA to hybridization probes.

Regarding such a streptavidin-based system the XNA on Gold™<sup>13</sup> affinity biochip developed by Thermohybrid, Germany, was tested. It employs the above described chemistry for the immobilization of biotinylated DNA. Preliminary results obtained with a linear mode MALDI-TOF mass spectrometer under non-optimized detection conditions suggested that specific and reproducible results can be obtained. Figure 7.18 shows a 6-plex hybridization result of a PCR amplified insert of a genomic DNA clone of known sequence that was recorded by means of a high-resolution reflector-mode MALDI-TOF mass spectrometer. However, despite conditions and instruments settings optimized for PNA detection, hybridization results could not be consistently reproduced, i.e. sometimes no signals were detected at all. In addition, as suggested by control experiments without immobilized DNA, unspecific binding of PNA probes, presumably to streptavidin, frequently occurred even in the presence of detergents, such as Tween-20. Hence, there was no guarantee that obtained results were sequence-dependent. The persisting problem of unspecificity of the XNA on Gold™ biochip was too crucial to follow up with this approach.

---

<sup>13</sup> <http://www.thermohybrid.com>



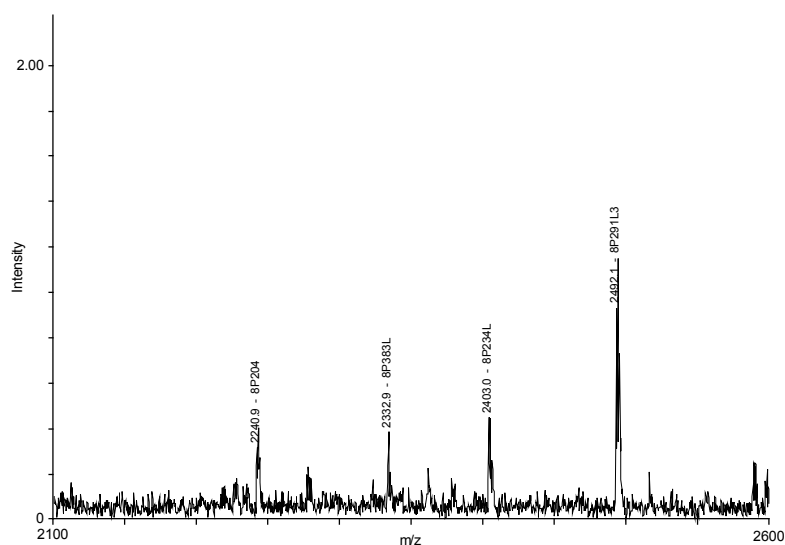


**Figure 7.18 6-plex PNA hybridization with a PCR product immobilized on a XNA on Gold™ biochip**

The MALDI-TOF mass spectrum shows the reproducible and specific hybridization result of four out of six different PNA octamers with a PCR product of known sequence.

#### 7.4.1.3 Nylon-based immobilization system

Unprecedented experience in conventional nylon membrane hybridizations and blotting gathered over the last three decades made it very reasonable to pursue the development of a nylon-based immobilization system. Furthermore, many studies have shown that for mass spectrometric analyses of proteins and protein digest different types of membranes can be applied for direct MALDI-TOF MS measurements (McComb et al., 1997, Worrall et al., 1998, Binz et al., 1999, Hung et al., 1999) supporting a nylon-based approach.

MALDI-TOF MS compatibility of such a nylon-based DNA immobilization system was demonstrated by the immobilization of DNA on small pieces of nylon membrane and subsequent multiplexed PNA hybridization. Following hybridization the membrane pieces were incubated with MALDI matrix solution III and mounted onto a modified MALDI target using double adhesive conductive tape (figure 7.19 A). For independent experiments under initial conditions reproducible results could be obtained suggesting that nylon membranes are suitable. To follow up with that approach, the development of a nylon-based DNA microarray was intensively pursued on the basis of industrial collaborations. A cooperation with Schleicher & Schuell Bioscience, USA, was initiated aiming at the further development of their nylon-based CAST™ slides towards MALDI-TOF-MS compatibility.

The CAST™ membrane was deposited on metal slides (Al or TiAlV<sub>6</sub> alloy) which proved to be a stable and adequate solution (figure 7.19 B). Such prepared slides were used for DNA immobilization and multiplexed PNA hybridization. Experiments with the metallic

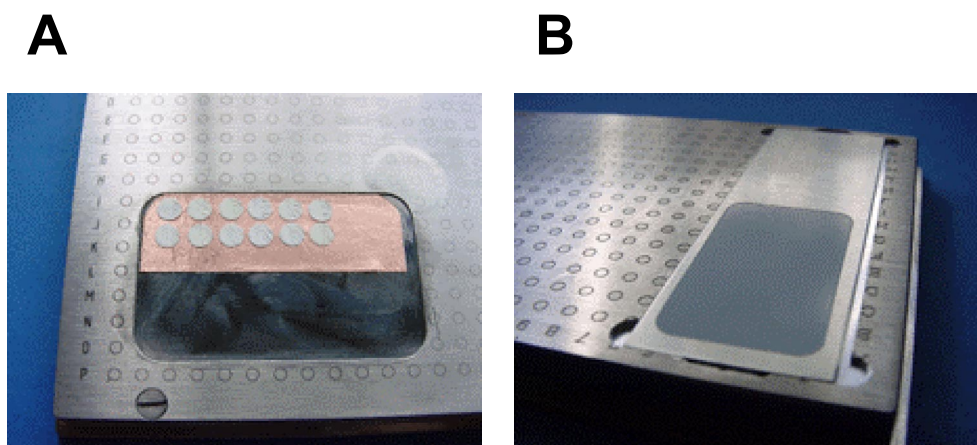


**Figure 7.19 Development of nylon-based immobilization system**

- A:** Milled conventional MALDI target with small pieces of nylon membranes (0,45  $\mu\text{m}$  pore size) of about 10  $\text{mm}^2$  size and that have been mounted on double adhesive conductive tape.
- B:** CAST™ membrane (0,45 $\mu\text{m}$  thick) on aluminum slide that has been mounted in the self-designed adapter.

CAST™ slides were reproducible and confirmed the preliminary results obtained with small pieces of nylon membrane (figure 7.20). However, signals were unspecific, resolution of signals was rather poor and hybridization results were not always detectable presumably due to membrane thickness and insufficient MALDI matrix crystallization. Less volatile matrix formulations, such as MALDI matrix solution III, on the other hand, improved the outcome. Experiments with CAST™ nylon membranes of smaller pore size (0,2  $\mu\text{m}$ ) and smaller membrane pieces did not improve results. Empirical observations revealed that signals were detected at the edges of a membrane piece rather than in the center. The evaluation of the FAST™ nitrocellulose membrane failed due to the chemical instability of nitrocellulose to organic solvents.

Despite the above mentioned problems, a nylon membrane based approach still remains promising once those drawbacks are overcome.

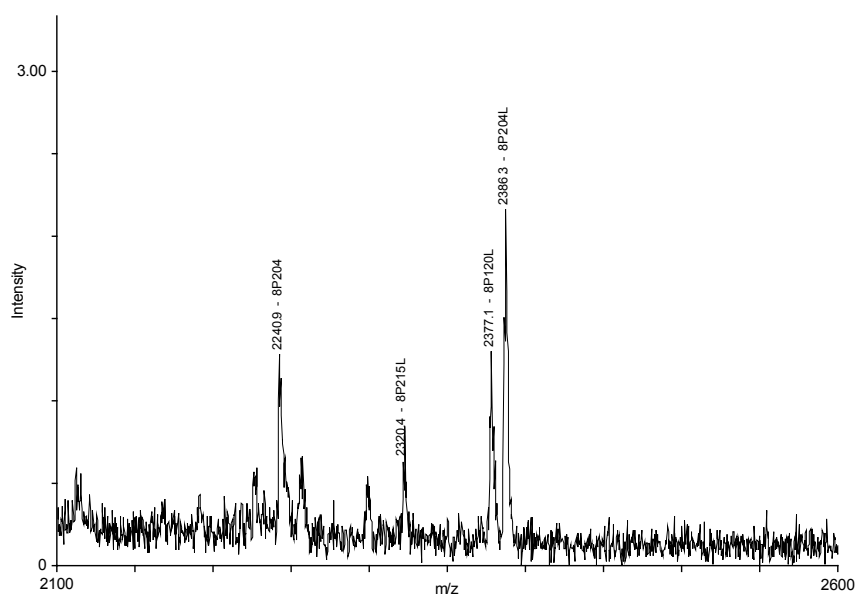


**Figure 7.20 6-plex PNA hybridization with a PCR product immobilized on a metallic CAST™ slide**

The MALDI-TOF mass spectrum shows the reproducible but unspecific hybridization result of four out of six different PNA octamers with a PCR product of known sequence.

#### 7.4.1.4 Dendritic immobilization system

Polyamidoamine (PAMAM) starburst dendrimers belong to polyfunctional dendritic linker systems that have been initially developed by Tomalia et al. (1980). Their suitability as pre-fabricated dendrimers for efficient DNA immobilization has been described by Benters et al. (2001, 2002) who demonstrated a 10-20 times higher DNA immobilization capacity compared to planar glass slides.

To exploit this feature for the concept of multiplexed OFP a collaboration with Chimera Biotec, Germany, who commercializes the PAMAM technology, was initialized. As a standard, PAMAM starburst dendrimers are applied on conventional glass slides. However, initial experiments with PAMAM functionalized silicon performed at Chimera suggested that a conductive silicon surface would be at least equally suitable. Therefore, it was decided to evaluate PAMAM functionalized silicon in comparison to conventional PAMAM glass slides. The latter were directly obtained from Chimera Biotec. In contrast, for the generation of PAMAM functionalized silicon doped silicon wafers were first polished, covered with a defined layer of thermally applied oxide (~ 1000 nm) and then cut into pieces of uniform glass slide format. Subsequently, PAMAM starburst dendrimers were applied as described (Benters et al., 2002). Two batches of silicon-based PAMAM

slides were produced of which the second one was methodically optimized. Figure 7.21 shows the reproducible hybridization result of a 6-plexed PNA hybridization with DNA immobilized on a conventional PAMAM glass slide (A) and PAMAM functionalized conductive silicon (B). Signal intensities yielded from silicon slides were consistently

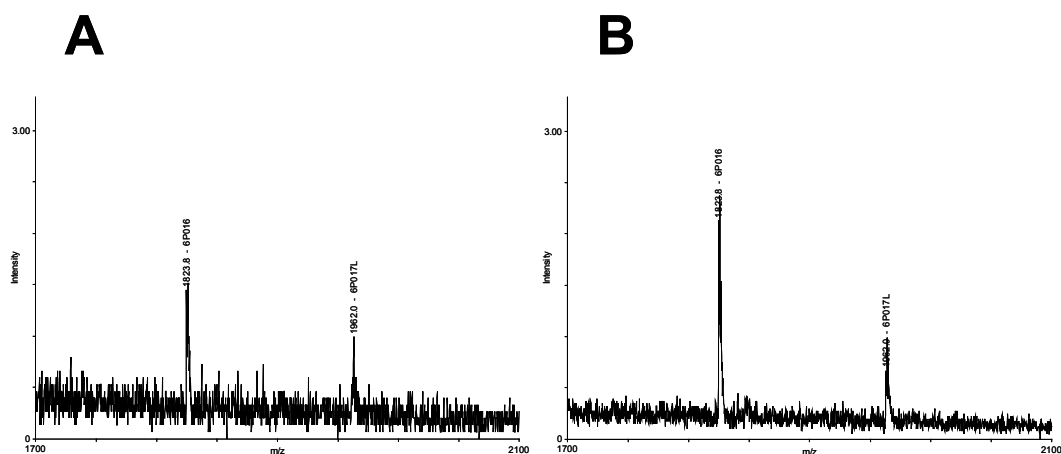


**Figure 7.21 6-plex PNA hybridization with a PCR product immobilized on PAMAM functionalized surfaces**

The MALDI-TOF mass spectra show the reproducible hybridization results of two out of four expected different PNA hexamers with a PCR product of known sequence immobilized on a conventional PAMAM glass slide (A) and PAMAM functionalized conductive silicon (B, second batch).

higher and showed a better resolution suggesting a superior performance compared to conventional non-conductive PAMAM glass slides. However, due to a lack of pre-structuring of the solid support an intricate on-slide sample localization occurred. Besides MALDI matrix crystallization appeared to be inconsistent resulting in impaired signal acquisition. Nevertheless, a PAMAM based dendritic immobilization system represents a powerful alternative once those challenges are overcome.

#### 7.4.2 Comparison of DNA immobilization systems

From the obtained results it became apparent that the success and quality of MALDI-TOF mass spectrometric measurements is highly dependent on MALDI matrix and sample crystallization. As for the evaluation of two immobilization systems, it is hence almost impossible to directly compare two microarray slides of different nature exclusively on the basis of hybridization signal intensities and resolution yielded by MALDI-TOF MS. Even

an excellent hybridization performance could be superimposed by an insufficient matrix crystallization resulting in very bad or no signals at all.

Consequently, to assess and compare their individual binding capacity the DNA immobilization systems tested in the course of this dissertation were evaluated with regard to their performance in fluorescent DNA hybridizations. Fluorescence intensities and signal-to-noise ratios simultaneously give information about DNA immobilization capacity as well as accessibility to hybridization probes. However, in contrast to direct labeling assays, where radioactively or fluorescence labeled DNA is used, it is not possible to determine the individual impact of one parameter separately. Nevertheless, the straightforwardness of the experimental setup and the rapidness of data acquisition compensate for this drawback. Furthermore, direct labeling assays do only provide information about one parameter at the same time. A simultaneous and separate determination of the influence of DNA immobilization capacity and accessibility is also unfeasible.

In the course of fluorescence DNA hybridization experiments the following immobilization systems were evaluated: streptavidin-based XNA on Gold™ biochip, metallic as well as conventional glass-based CAST™ nylon membrane slides, PAMAM functionalized conductive silicon (initial and refined batch) as well as conventional PAMAM glass slides, and Quantifoil QMT™ aldehyde glass. Figure 7.22 shows the highly reproducible hybridization results of a Cy-3 fluorescence labeled DNA oligonucleotide complementary to a PCR priming region that was hybridized to PCR amplified DNA of different size. Results of the XNA on Gold™ biochip and the conventional glass-based membrane slide are not illustrated. The latter yielded unsatisfactory results as did the metallic CAST™ slide (fig. 7.22 A) whereas the former failed to deliver any meaningful data. Both findings can be explained as follows: Gold which forms the basis of the streptavidin-based XNA chip is known to quench fluorescence thereby eliminating any fluorescent signal. In fact, only weak signals at high DNA concentrations could be detected. Nylon membranes, as already mentioned before, act as a sponge resulting in a spread of DNA applied which caused smeared fluorescence signals.

Figure 7.23 shows the numeric analysis of fluorescence hybridization results of the DNA microarrays that could be analyzed using the GenePix Pro 4.1 software package. From the figure it is apparent that increasing DNA concentrations lead to higher overall signal intensities and slightly improved signal-to-noise ratios. Besides, within the range of the applied dilution series of spotted DNA concentrations no plateau seems to be reached. As expected, DNA of decreasing length yields increasing hybridization signal intensities which are due to higher numbers of molecules arrayed per given concentration unit. All spotted slides showed an increase in fluorescent signal intensities as a function of

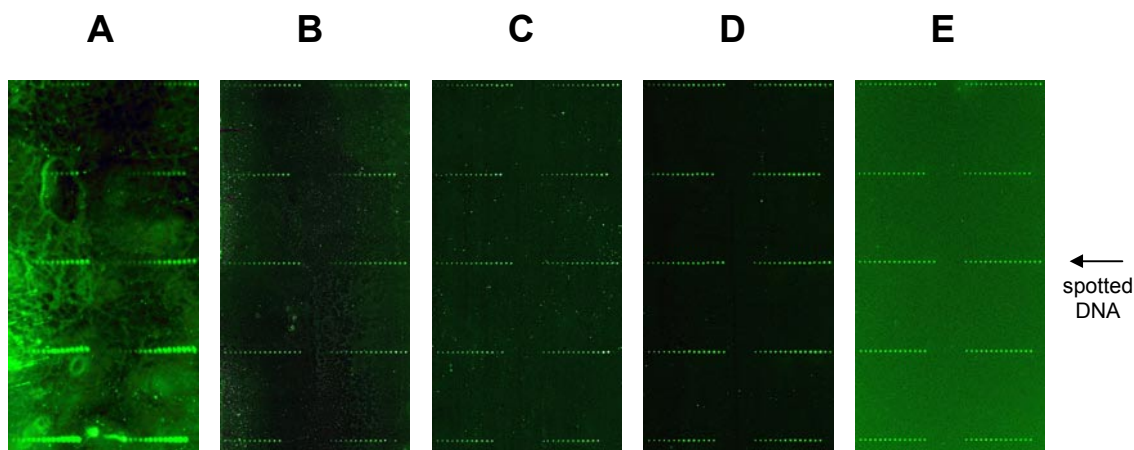


**Figure 7.22 Comparison of DNA microarrays hybridized with a fluorescent DNA probe**

DNA microarrays were spotted, processed, subsequently hybridized with a Cy-3 fluorescence labeled DNA 18mer oligonucleotide and scanned as described in chapter 6.11. Microarrays on the following solid supports are depicted: metallic CAST™ nylon membrane slide (**A**), PAMAM functionalized conductive silicon initial (**B**) and refined batch (**C**), conventional PAMAM glass slide (**D**), and Quantifoil QMT™ aldehyde glass slide (**E**). PCR amplified DNA of five different lengths (450 bp, 650 bp, 1060 bp, 1350 bp, 1520 bp) was spotted as a dilution series (25, 50, 100, 200, 400, 600, 800, 1000 ng/μL). Each row represents a specific PCR product that was arrayed with increasing concentrations (from left to right) in adjacent duplicates and duplicate subarrays (horizontally neighboring rows). DNA length decreases from top rows (1520 bp) to bottom rows (450 bp). Fluorescence at  $\lambda=532$  nm was scanned with a PMT voltage of 550.

the applied dilution series, except Quantifoil aldehyde slides, which behaved conversely. Considering the different immobilization systems, it appears that PAMAM functionalized silicon is by far superior to glass based attachment chemistries. Noticeably, slides of the methodically refined silicon batch perform considerably better than slides of the initial batch. There is, however, only little difference in performance between PAMAM glass and Quantifoil aldehyde glass slides.

## 7. Results

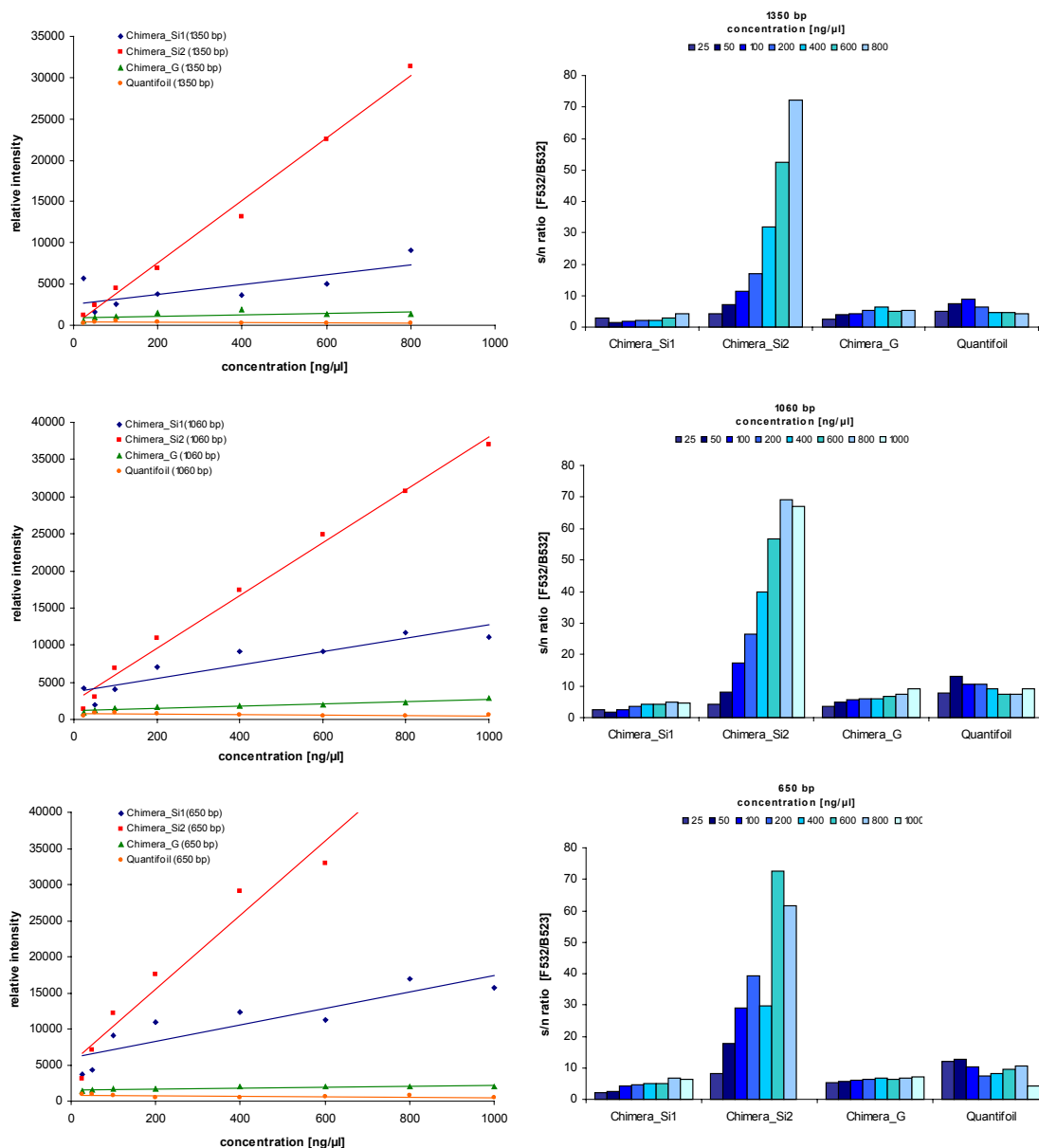


**Figure 7.23** Numeric analysis of fluorescence DNA hybridization results

The results of numeric analysis of fluorescence DNA hybridizations of three different DNA lengths (1350 bp, 1060 bp, 650 bp) gained on PAMAM functionalized silicon initial batch (Chimera\_Si1) and refined batch (Chimera\_Si2) as well as PAMAM functionalized glass slides (Chimera\_G) and Quantifoil QMT™ aldehyde glass slides (Quantifoil) are depicted. On the left, normalized relative fluorescence signal intensities in dependence of spotted DNA concentration are shown for the respective microarrays. On the right, signal-to-noise ratios for each slide under investigation are given, in turn, in dependence of spotted DNA concentration.